National Library of Canada

Acquisitions and Bibliographic Services Branch

395 Wellington Street
Ottawa, Ontario
K1A 0N4

Bibliothèque nationale du Canada

Direction des acquisitions et des services bibliographiques

395, rue Wellington
Ottawa (Ontario)
K1A 0N4

Your file Votre référence

Our file Notre référence

NOTICE

The quality of this microform is heavily dependent upon the quality of the original thesis submitted for microfilming. Every effort has been made to ensure the highest quality of reproduction possible.

If pages are missing, contact the university which granted the degree.

Some pages may have indistinct print especially if the original pages were typed with a poor typewriter ribbon or if the university sent us an inferior photocopy.

AVIS

La qualité de cette microforme dépend grandement de la qualité de la thèse soumise au microfilmage. Nous avons tout fait pour assurer une qualité supérieure de reproduction.

S'il manque des pages, veuillez communiquer avec l'université qui a conféré le grade.

La qualité d'impression de certaines pages peut laisser à désirer, surtout si les pages originales ont été dactylographiées à l'aide d'un ruban usé ou si l'université nous a fait parvenir une photocopie de qualité inférieure.

Canada

Isolation, Immortalization, and Characterization of Rabbit Cortical Collecting Duct Cells which Express AT_1 Angiotensin II Receptors

by
Laura Regnier

Thesis submitted for the degree of
Masters of Science from
the Department of Physiology
Faculty of Medicine
University of Ottawa

May 1995

ISBN 0-612-04971-X

Canada

Nom _____

Dissertation Abstracts International est organisé en catégories de sujets. Veuillez s.v.p. choisir le sujet qui décrit le mieux votre thèse et inscrivez le code numérique approprié dans l'espace réservé ci-dessous.

_____ ☐☐☐☐ U·M·I

SUJET CODE DE SUJET

Catégories par sujets

HUMANITÉS ET SCIENCES SOCIALES

COMMUNICATIONS ET LES ARTS
Architecture 0729
Beaux-arts 0357
Bibliothéconomie 0399
Cinéma 0900
Communication verbale 0459
Communications 0708
Danse 0378
Histoire de l'art 0377
Journalisme 0391
Musique 0413
Sciences de l'information 0723
Théâtre 0465

ÉDUCATION
Généralités 515
Administration 0514
Art 0273
Collèges communautaires 0275
Commerce 0688
Économie domestique 0278
Éducation permanente 0516
Éducation préscolaire 0518
Éducation sanitaire 0680
Enseignement agricole 0517
Enseignement bilingue et multiculturel 0282
Enseignement industriel 0521
Enseignement primaire 0524
Enseignement professionnel 0747
Enseignement religieux 0527
Enseignement secondaire 0533
Enseignement spécial 0529
Enseignement supérieur 0745
Évaluation 0288
Finances 0277
Formation des enseignants 0530
Histoire de l'éducation 0520
Langues et littérature 0279
Lecture 0535
Mathématiques 0280
Musique 0522
Orientation et consultation 0519
Philosophie de l'éducation 0998
Physique 0523
Programmes d'études et enseignement 0727
Psychologie 0525
Sciences 0714
Sciences sociales 0534
Sociologie de l'éducation 0340
Technologie 0710

LANGUE, LITTÉRATURE ET LINGUISTIQUE
Langues
- Généralités 0679
- Anciennes 0289
- Linguistique 0290
- Modernes 0291

Littérature
- Généralités 0401
- Anciennes 0294
- Comparée 0295
- Médiévale 0297
- Moderne 0298
- Africaine 0316
- Américaine 0591
- Anglaise 0593
- Asiatique 0305
- Canadienne (Anglaise) 0352
- Canadienne (Française) 0355
- Germanique 0311
- Latino-américaine 0312
- Moyen-orientale 0315
- Romane 0313
- Slave et est-européenne 0314

PHILOSOPHIE, RELIGION ET THÉOLOGIE
Philosophie 0422
Religion
- Généralités 0318
- Clergé 0319
- Études bibliques 0321
- Histoire des religions 0320
- Philosophie de la religion 0322

Théologie 0469

SCIENCES SOCIALES
Anthropologie
- Archéologie 0324
- Culturelle 0326
- Physique 0327

Droit 0398
Économie
- Généralités 0501
- Commerce-Affaires 0505
- Économie agricole 0503
- Économie du travail 0510
- Finances 0508
- Histoire 0509
- Théorie 0511

Études américaines 0323
Études canadiennes 0385
Études féministes 0453
Folklore 0358
Géographie 0366
Gérontologie 0351
Gestion des affaires
- Généralités 0310
- Administration 0454
- Banques 0770
- Comptabilité 0272
- Marketing 0338

Histoire
- Histoire générale 0578
- Ancienne 0579
- Médiévale 0581
- Moderne 0582
- Histoire des noirs 0328
- Africaine 0331
- Canadienne 0334
- États-Unis 0337
- Européenne 0335
- Moyen-orientale 0333
- Latino-américaine 0336
- Asie, Australie et Océanie 0332

Histoire des sciences 0585
Loisirs 0814
Planification urbaine et régionale 0999
Science politique
- Généralités 0615
- Administration publique 0617
- Droit et relations internationales 0616

Sociologie
- Généralités 0626
- Aide et bien-être social 0630
- Criminologie et établissements pénitentiaires 0627
- Démographie 0938
- Études de l'individu et de la famille 0628
- Études des relations interethniques et des relations raciales 0631
- Structure et développement social 0700
- Théorie et méthodes 0344
- Travail et relations industrielles 0629

Transports 0709
Travail social 0452

SCIENCES ET INGÉNIERIE

SCIENCES BIOLOGIQUES
Agriculture
- Généralités 0473
- Agronomie 0285
- Alimentation et technologie alimentaire 0359
- Culture 0479
- Élevage et alimentation 0475
- Exploitation des pâturages 0777
- Pathologie animale 0476
- Pathologie végétale 0480
- Physiologie végétale 0817
- Sylviculture et faune 0478
- Technologie du bois 0746

Biologie
- Généralités 0306
- Anatomie 0287
- Biologie (Statistiques) 0308
- Biologie moléculaire 0307
- Botanique 0309
- Cellule 0379
- Écologie 0329
- Entomologie 0353
- Génétique 0369
- Limnologie 0793
- Microbiologie 0410
- Neurologie 0317
- Océanographie 0416
- Physiologie 0433
- Radiation 0821
- Science vétérinaire 0778
- Zoologie 0472

Biophysique
- Généralités 0786
- Médicale 0760

SCIENCES DE LA TERRE
Biogéochimie 0425
Géochimie 0996
Géodésie 0370
Géographie physique 0368
Géologie 0372
Géophysique 0373
Hydrologie 0388
Minéralogie 0411
Océanographie physique 0415
Paléobotanique 0345
Paléoécologie 0426
Paléontologie 0418
Paléozoologie 0985
Palynologie 0427

SCIENCES DE LA SANTÉ ET DE L'ENVIRONNEMENT
Économie domestique 0386
Sciences de l'environnement 0768
Sciences de la santé
- Généralités 0566
- Administration des hôpitaux 0769
- Alimentation et nutrition 0570
- Audiologie 0300
- Chimiothérapie 0992
- Dentisterie 0567
- Développement humain 0758
- Enseignement 0350
- Immunologie 0982
- Loisirs 0575
- Médecine du travail et thérapie 0354
- Médecine et chirurgie 0564
- Obstétrique et gynécologie 0380
- Ophtalmologie 0381
- Orthophonie 0460
- Pathologie 0571
- Pharmacie 0572
- Pharmacologie 0419
- Physiothérapie 0382
- Radiologie 0574
- Santé mentale 0347
- Santé publique 0573
- Soins infirmiers 0569
- Toxicologie 0383

SCIENCES PHYSIQUES
Sciences Pures
Chimie
- Généralités 0485
- Biochimie 487
- Chimie agricole 0749
- Chimie analytique 0486
- Chimie minérale 0488
- Chimie nucléaire 0738
- Chimie organique 0490
- Chimie pharmaceutique 0491
- Physique 0494
- PolymÈres 0495
- Radiation 0754

Mathématiques 0405
Physique
- Généralités 0605
- Acoustique 0986
- Astronomie et astrophysique 0606
- Électronique et électricité 0607
- Fluides et plasma 0759
- Météorologie 0608
- Optique 0752
- Particules (Physique nucléaire) 0798
- Physique atomique 0748
- Physique de l'état solide 0611
- Physique moléculaire 0609
- Physique nucléaire 0610
- Radiation 0756

Statistiques 0463

Sciences Appliqués Et Technologie
Informatique 0984
Ingénierie
- Généralités 0537
- Agricole 0539
- Automobile 0540
- Biomédicale 0541
- Chaleur et thermodynamique 0348
- Conditionnement (Emballage) 0549
- Génie aérospatial 0538
- Génie chimique 0542
- Génie civil 0543
- Génie électronique et électrique 0544
- Génie industriel 0546
- Génie mécanique 0548
- Génie nucléaire 0552
- Ingénierie des systèmes 0790
- Mécanique navale 0547
- Métallurgie 0743
- Science des matériaux 0794
- Technique du pétrole 0765
- Technique minière 0551
- Techniques sanitaires et municipales 0554
- Technologie hydraulique 0545

Mécanique appliquée 0346
Géotechnologie 0428
Matières plastiques (Technologie) 0795
Recherche opérationnelle 0796
Textiles et tissus (Technologie) 0794

PSYCHOLOGIE
Généralités 0621
Personnalité 0625
Psychobiologie 0349
Psychologie clinique 0622
Psychologie du comportement 0384
Psychologie du développement 0620
Psychologie expérimentale 0623
Psychologie industrielle 0624
Psychologie physiologique 0989
Psychologie sociale 0451
Psychométrie 0632

UNIVERSITÉ D'OTTAWA
UNIVERSITY OF OTTAWA

DEDICATION

To my loving parents Mary-Jane and Zephyr Regnier

DECLARATION

I certify that this thesis does not incorporate without acknowledgement any material previously submitted for a degree in any University. To the best of my knowledge and belief, this thesis does not contain any material previously published or written by another except where due reference is made in text.

I authorize the University of Ottawa to reproduce this thesis in total or in part at the request of another institution, for academic research.

Laura Regnier

ACKNOWLEDGMENTS

First and foremost, I would like to thank my supervisor, Professor Richard L. Hébert for welcoming me into his laboratory and for giving me the wonderful opportunity to do research. His support and guidance throughout are greatly appreciated.

I would also like to express deep gratitude to Dr. Kevin D. Burns for his constant encouragement and his contributions which made the realisation of this project possible. Special thanks to both Dr. Kevin D. Burns and Professor Linda N. Peterson for being members of my advisory committee.

Many thanks to Professor William Staines for his time, his generosity and insightful discussions throughout.

I would also like to thank my fellow students and friends Agnès Roczniak, Chris Kennedy, Chris Naismith, Tracey Kennedy, Tim O'Connor and Nicholas Argent for their help and their encouragement.

Finally, I would like to thank my family for their patience, their support and their love.

ABSTRACT

Isolation, Immortalization, and Characterization of Rabbit Cortical Collecting Duct Cells which Express AT_1 Angiotensin II Receptors

Functions of angiotensin II (Ang II) in distal nephron are poorly understood. To study Ang II signalling in cortical collecting duct (CCD), CCD cells were immortalized by transfection with a plasmid encoding the large T antigen of SV40. Hormone-induced (10^{-7} M) cAMP responses were characteristic of intact CCD: arginine vasopressin (AVP) and prostaglandin E_2 (PGE_2) significantly stimulated cAMP production, while parathyroid hormone (PTH) and salmon calcitonin (sCT) had no effect. Scanning electron microscopy (SEM) revealed cells with apical microplicae characteristic of α-intercalated cells (α-IC); other cells had few blunt microvilli consistent with either principal cells (PC) or ß-intercalated cells (ß-IC). Approximately 27% of transfected cells bound the rabbit ß-IC marker peanut lectin agglutinin. Antibodies directed against surface antigens of PC (mAb 703) and IC (mAb 503), immunolabelled up to 26% of cells. In transfected cells, a single class of Ang II receptors (K_d=0.78 nM) was detected by radioligand binding, and AT_1 Ang II receptor mRNA was demonstrated by Northern analysis. Ang II (10^{-7} M) inhibited AVP-stimulated cAMP production, and low concentrations of Ang II (10^{-12} M) significantly increased phosphoinositide hydrolysis. Thus, we immortalized a rabbit CCD cell line that retains characteristic morphological and hormonal properties. These cells express AT_1 Ang II receptors linked to inhibition of cAMP formation and to activation of phospholipase C. Coupling of Ang II receptors to these pathways may modulate CCD transport and growth.

TABLE OF CONTENTS

LIST OF TABLES

LIST OF FIGURES

LIST OF ABBREVIATIONS

AC	Adenylate cyclase
ACE	Angiotensin converting enzyme
Ang II	Angiotensin II
AT_1, AT_2	Angiotensin receptor subtypes
AVP	Arginine vasopressin
B1	First band of Ficoll gradient
BCIP	5-bromo-4-chloro-3-indolyl-phosphate-4-toluisin salt
BLIP	Basolateral integral protein (water channel)
B_{max}	Maximal binding
BSA	Bovine Serum Albumin
cAMP	Cyclic adenosine monophosphate
cGMP	Cyclic guanosine monophosphate
CCD	Cortical collecting duct
cDNA	Complimentary DNA
Ci, mCi, μCi	Curie, millicurie, microcurie
cpm	Counts per minute
CTL	Control
DAG	Diacylglycerol
dCTP	Deoxy cytosine trisphosphate
ddH_2O	Double distilled H_2O
DEPC	Diethyl pyrocarbonate
DMEM/HamF12	Dulbecco's modified Eagle medium, Ham F12
DMSO	Dimethyl sulfoxide
DNA	Deoxyribonucleic acid
EC_{50}	Dose causing half maximal stimulation
EDTA	Ethylenediamine tetraacetic acid
EP_1, EP_2, EP_3, EP_4	E prostanoid receptor subtypes
FBS	Fetal bovine serum
FITC	Fluorescein isothyocyanate
FLB	Formaldehyde loading buffer
g	Gravitational force
g, mg, μg	Gram, milligram, microgram
G_i	Inhibitory G protein
G_s	Stimulatory G protein
^3H	Tritium
HEBS	Hepes-buffered saline
IBMX	Isobutyl methyl xanthine
α-IC, ß-IC, γ-IC	Alpha, Beta, Gamma intercalated cell
Ig	Immunoglobulin
IP_1, IP_2, IP_3	Inositol phosphate
kb	Kilobase

K_d	Dissociation constant
KHS	Krebs-Heinseleit solution
KHSB	Krebs-Heinseleit solution containing BSA
M, mM, μM, pM	Molar, millimolar, micromolar, picomolar
mAb	Monoclonal antibody
MDCK	Madin-Darby canine kidney cell line
min	Minutes
MOPS	3-(N-morpholino) propanesulfonic acid
mRNA	Messenger RNA
n	Number of observations
N	Normality
NBT	4-nitro-blue-tetrazolium chloride
O.D.	Optical density
oligo(dT)	Oligo deoxythymidine
PBS	Phosphate buffered saline
PGE_2	Prostaglandin E_2
PC	Principal cell
PKA, PKC	Protein kinase A, C
PI	Phosphoinositide
PIP_2	Phosphatidylinositol-4,5-bisphosphate
PLA_2, PLC, PLD	Phospholipase A_2, C, D
PNA	Peanut lectin agglutinin
Poly $(A)^+$	Poly adenosine
PTH	Parathyroid Hormone
RAS	Renin-angiotensin system
RIA	Radioimmunoassay
RNA	Ribonucleic acid
rRNA	Ribosomal RNA
sCT	Salmon calcitonin
SDS	Sodium dodecyl sulphate
sH_2O	Sterile H_2O
SSC	Sodium chloride sodium citrate
SV40	Simian virus 40
SEM	Scanning electron microscopy
SEM	Standard error mean
SLP	Sulprostone
T_3	3,3',5-Triiodo-L-thyronine
TCA	Trichloro acetic acid
TE	Tris-EDTA
TEM	Transmission electron microscopy
tRNA	Transfer RNA
V_1, V_2	Vasopressin receptor subtypes
WCH-CD	Collecting duct water channel

CHAPTER 1

THE CORTICAL COLLECTING DUCT

1.0 Introduction

Starling praised the kidney as having "a power of adaptation which almost gives one the idea that its component parts must be endowed with intelligence" (Starling 1909). Indeed, the kidney is capable of maintaining homeostasis under extreme conditions. This capacity is a credit to the phenomenal architecture of the kidney which allows for a unique distribution of labour within each individual nephron.

The nephron is divided into segments which are structurally and functionally distinct. The final segment of the nephron, the collecting duct, is in itself heterogenous along its length. Collecting ducts are classified by their location within the kidney: cortical, outer medullary (outer stripe and inner stripe), and inner medullary segments (Figure 1.0) (Lefurgey et al. 1979).

Being composed of several different cell types, the collecting duct is capable of numerous transport functions. In fact, the collecting duct is an important site of sodium, water and bicarbonate transport. The cell types involved in these electrolyte transport processes are principal cells (PC) and intercalated cells (α-IC, ß-IC). The following discussion will focus on the morphological and functional properties of PC, α-IC and ß-IC, as well as the factors which influence these characteristics.

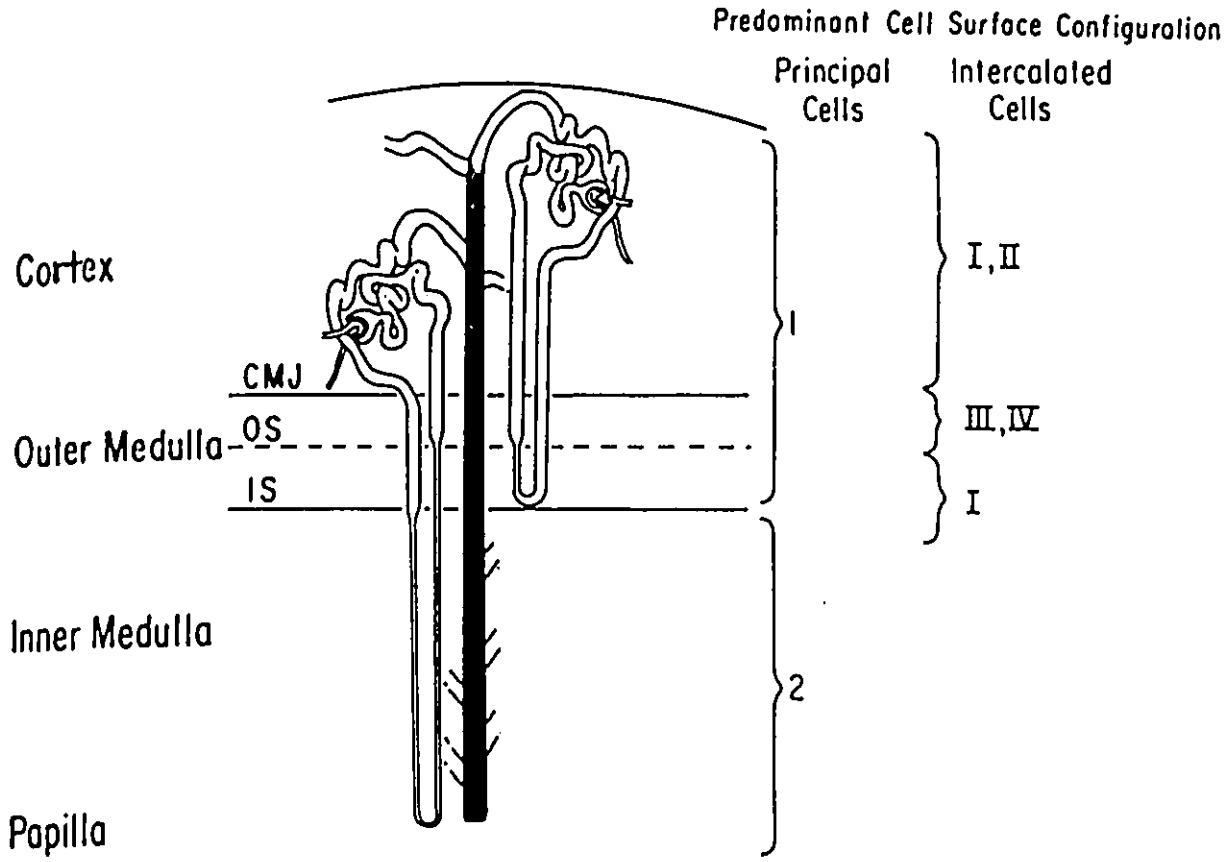

Figure 1.0

The collecting duct. The collecting duct begins beyond the first junction of one tubule with another and extends from cortex to papilla (in black). At right is the distribution of the two surface types observed in principal cells and the four surface patterns noted in the intercalated cells (see text for more detail). Figure reproduced from Lefurgey et al. 1979.

1.1 Principal Cell Ultrastructure

The principal cell is the predominant cell type of the collecting duct and comprises about two thirds of the total cell population. The morphology of these cells has been well described by electron microscopy. Using scanning electron microscopy (SEM) Lefurgey and Tisher (1979) described two morphological configurations of rabbit PC. PC occurring in the cortical and outer medullary regions displayed a single central cilium and widely spaced short microvilli. PC located in the inner medullary and papillary regions also displayed a single cilium, however, the apical membrane was packed with abundant short microvilli. Laterally, the cells interlocked by small finger-like villi that extended into the intercellular space. Studies measuring the PC cell dimensions revealed that the overall shape of the cells is hexagonal (Kaissling et al. 1979, Welling et al. 1981, O'Neil et al. 1985). The same observations were made by Evan et al. (1991) confirming that the apical surface of PC have scattered short microvilli, a centrally placed cilium and a hexagonal shape.

Transmission electron microscopy (TEM) revealed that principal cells lining the outer, mid, and inner cortical collecting duct have few cytoplasmic organelles and pale-staining cytoplasm. A well-developed basal labyrinth composed of numerous infoldings of the lateral and basal plasmalemma is a prominent feature of principal cells and may be related to function (LeFurgey et al. 1979). In this regard, the extensive infoldings of the PC basolateral labyrinth offer a large surface area for optimal transporting capacity. Other characteristics included a large apical spherical nucleus, small mitochondria, and many small Golgi distributed all over the cell. Lysosomes, lipid droplets and glycogen were found to occur to varying extents. The rough endoplasmic reticulum is sparse whereas the smooth

endoplasmic reticulum is well developed (Kaissling et al. 1979). Microtubules and microfilaments form a dense cytoskeletal meshwork below the apical membrane. "Aggrephores" composed of vesicles located beneath the apical membrane may contain water channels (Hays et al. 1987). In tubules, these cells occurred adjacent to each other with interdigitation of lateral cell membranes (Ridderstrale et al. 1988, Verlander et al. 1987, Evan et al. 1991).

1.2 Intercalated Cell Ultrastructure

Comprising about one third of the total cell population, intercalated cells are divided into two subtypes: α-intercalated (α-IC) and ß-intercalated (ß-IC). The term "intercalated" originates from the observation that these cells never occur adjacent to each other; rather they occur interspersed or "intercalated" between connecting tubule cells in the connecting tubule and principal cells in the CCD. Their abundance relative to principal cells in the cortical collecting duct is approximately 2:3 in rat and rabbit (Kaissling et al. 1979).

IC have been well characterized by SEM and TEM. In contrast to the PC, the cellular outline of the IC is more round or oval than polygonal (Welling et al. 1981, O'Neil et al. 1985). An extensively amplified apical membrane is the most prominent characteristic of these cells. Lefurgey and Tisher (1979) described four configurations of the apical cell surface of intercalated cells by SEM. The type I cells possessed abundant short microvilli whereas type II cells possessed both short and long microvilli. The type III cells possessed only microplicae in contrast to the type IV which displayed both microplicae and microvilli. The distribution of these surface patterns is depicted in Figure 1. The differences among

the various manifestations are often subtle and gradual with many intermediate variations. These variations may represent several specific subtypes of intercalated cells or functional and maturational variations of a single cell line. There is evidence to suggest that the microplicated IC is an α-IC whereas the IC displaying only microvilli is a ß-IC (Evan et al. 1991, Verlander et al. 1987). Freeze fracture studies have demonstrated clusters of rod shaped particles (studs) on both the luminal and basolateral membranes of all IC cells in the CCD (Ridderstrale et al. 1988). These studs correspond to integral membrane proteins whose distribution is congruent with that of H^+-ATPase in the CCD (Ridderstrale et al. 1988) and the H^+,K^+-ATPase of the outer medullary collecting duct (OMCD) (Stetson et al. 1980).

TEM revealed that the cytoplasm of the IC is dark-staining and contains an abundance of cytoplasmic organelles including numerous mitochondria causing the large apical cell pole to protrude into the lumen. They also possess abundant vesicles and vacuoles beneath the apical membrane. A dense, meshed, smooth endoplasmic reticulum and a well-developed Golgi apparatus occupy a large area in the cell (Kaissling et al. 1979, LeFurgey et al. 1979, Ridderstrale et al. 1988, Verlander et al. 1987, Evan et al. 1991).

The fact that both principal cells and intercalated cells, exhibit more than one phenotype may reflect different functional states of these cells. Otherwise, these variations may represent several specific types of principal and intercalated cells or functional and maturational variations of a single cell line. On the other hand, cell surface specializations may be transient, that is, continually forming and reforming in response to varying physiologic phenomena (see section on modulation of structure and function).

1.3 Principal Cell Function

Principal cells are primarily involved in sodium (Na^+) and water reabsorption and potassium (K^+) secretion (Figure 1.1) (Stokes 1993). Because the intracellular Na^+ concentration is low (10 mM) and the inside of the cell is negative with respect to the lumen, an electrochemical gradient favors the entry of Na^+ via luminal (apical) membrane Na^+ channels. The Na^+ that enters the cell is extruded via a basolateral Na^+-K^+ ATPase which exchanges $3Na^+$ for $2K^+$ (Fejes-Tóth et al. 1989). Aldosterone enhances the activity and the expression of the Na^+-K^+-ATPase (Minuth et al. 1987). The expression of this pump can be detected with antibodies directed against the α-subunit of Na^+-K^+-ATPase which strictly recognize the basolateral membrane of mature principal cells in the CCD (Minuth et al. 1987). Most of the K^+ entering the cell via the pump exits the cell at the apical membrane and is excreted in urine. A fraction of K^+ leaves the cell via the basolateral membrane and is "recycled". Chloride can diffuse into and out of a basolateral membrane channel (Stokes 1993). The physiologic relevance of chloride recycling remains obscure.

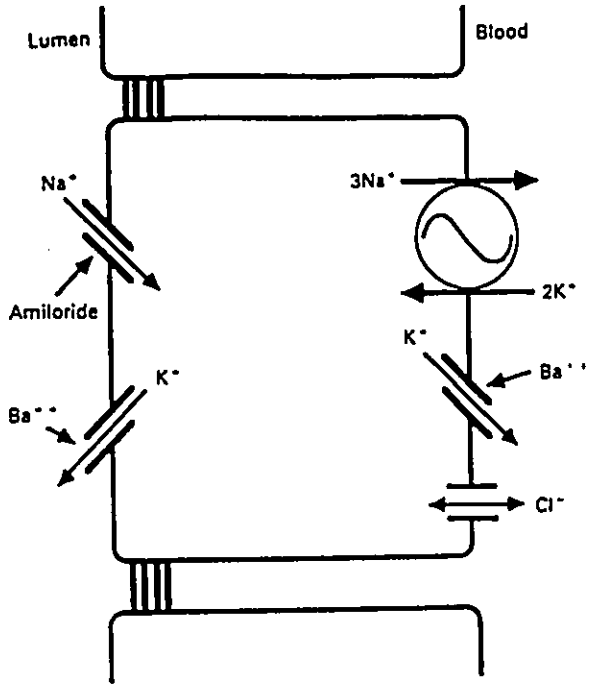

Figure 1.1

Principal cells of rabbit CCD. Schematic diagram depicting the apical and basolateral distribution of channels and ion exchangers. Figure reproduced from Stokes 1993.

Principal cells of the collecting duct are the primary targets of antidiuretic hormone (ADH) also known as vasopressin (Brown et al. 1983, Kirk 1988). This hormone stimulates water reabsorption when it binds to basolateral V2 receptors. V2 receptors couple to stimulatory G proteins, initiate the adenylate cyclase-mediated signalling cascade, which results in increased cAMP generation and activation of cAMP dependent protein kinase (PKA) (Snyder et al. 1992). This cascade triggers insertion of water channels (WCH-CD) into the luminal membrane, causing increased water permeability of the apical epithelial membrane of the collecting duct (Breyer et al. 1994a, Kishore et al. 1995). Vasopressin also

stimulates Na^+ and K^+ secretion in these cells but this effect is transient (Schafer et al. 1990, Wang et al. 1992).

The vasopressin V1 receptor subtype has also been identified on the apical and basolateral membranes of principal cells (Bunatowska-Hledin et al. 1989). This receptor is coupled to phospholipase C (PLC) which catalyses the breakdown of phosphatidylinositol-4,5-bisphosphate (PIP_2) to inositol 1,4,5-trisphosphate (IP_3) and diacylglycerol with the resultant mobilization of calcium and activation of protein kinase C (PKC), respectively (Ausiello et al. 1987). Stimulation of the major V1 signalling pathways, appear to inhibit AVP-stimulated water flow, suggesting that AVP might inhibit its own V2-mediated hydroosmotic effect via V1 receptors (Breyer 1991).

Similarly, PGE_2 has been demonstrated to inhibit vasopressin- stimulated water flow (Hébert et al. 1990). This effect has been attributed to the binding of PGE_2 to basolateral EP_3 receptor subtypes. These receptors are linked to inhibitory G proteins (Gi) which inhibit adenylate cyclase activity and ultimately suppress water permeability.

In contrast, in the absence of vasopressin, PGE_2 binds EP_2 receptor subtypes which are coupled to stimulatory G proteins linked to adenylate cyclase thus increasing cAMP formation and subsequently, increasing water transport (Hébert et al. 1990).

The EP_1 receptor subtype is coupled to the PLC pathway. Studies utilizing staurosporine showed that PGE_2 mediated inhibition of vasopressin induced water flow is associated with PKC activation (Hébert et al. 1990, Hébert et al. 1991).

Thus, PGE_2 exerts its effects on the collecting duct through the EP_1, EP_2, and EP_3, "E" prostanoid receptor subtypes. An EP_4 receptor subtype has also been proposed (Breyer

et al. 1994b). Several receptor subtype specific analogues have been developed in order to examine the functional effects of each individual receptor subtype on the CCD, these include: EP_2 receptor selective analogues, butaprost, 19-(R)-OH-PGE_2, and the EP_3 receptor selective analogue sulprostone (Breyer et al. 1994, Woodward et al. 1993, Hébert 1993).

Considering the functional effects of PGE_2 in the CCD it is important to note that the collecting duct is the major renal site of action of this autacoid and that PGE_2 production is stimulated by vasopressin itself (Bonvalet et al. 1987).

1.4 Intercalated Cell Function

The fact that IC contain large amounts of the enzyme carbonic anhydrase was a major indication of their possible involvement in acid-base regulation.

The primary function of the α-IC is proton secretion. It accomplishes this task by means of three major transporters (Figure 1.2) (Stokes 1993). An H^+-ATPase on the apical membrane translocates H^+ from the cell cytoplasm into the lumen. This electrogenic H^+-ATPase is an isoform of the vacuolar H^+-ATPase (Nelson et al. 1992), and can be identified with antibodies to subunits of this enzyme, a method used to immunohistochemically identify intercalated cells (Verlander et al. 1994(a), Bastani et al. 1994, Alper et al. 1989). HCO_3^- generated during this process is extruded by a basolateral electroneutral anion exchanger. The anion exchanger is similar to the erythroid band 3 anion exchanger and is recognized by antibodies to band 3 (Schuster et al. 1991, Verlander et al. 1994 (b), Schuster et al. 1986). The Cl^- that enters the cell via the anion exchanger is recycled through a basolateral Cl^- channel. α-IC lose the ability to secrete protons when the anion exchanger

is inhibited by disulfonic stilbenes (DIDS) (Stone et al. 1983).

In contrast to the α-IC, the primary function of ß-IC is luminal HCO_3^- secretion (Figure 1.2) (Stokes 1993). This process involves an apical anion exchanger that secretes HCO_3^- into the lumen in exchange for Cl^- which subsequently exits the cell via a basolateral Cl^- channel. The anion exchanger is stimulated by HCO_3^- produced by a basolateral H^+-ATPase (Verlander et al. 1994 (a)). Initial attempts to identify the anion exchanger in the ß-IC cells failed when the erythroid band 3 antibody was unreactive with ß-IC (Schuster et al. 1986, Schuster et al. 1991). More recently, van Adelsberg (1993, 1994) utilized cultured rabbit ß-IC to suggest that the apical Cl^-/HCO_3^- exchanger was in fact band 3. This has not been confirmed.

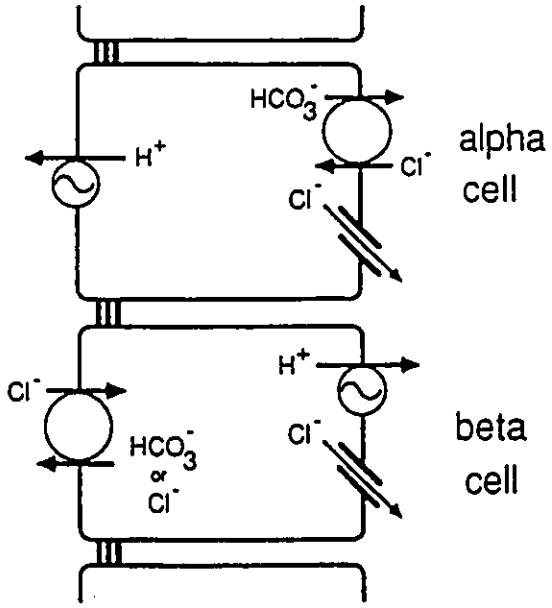

Figure 1.2

Intercalated cells of the rabbit CCD. The apical and basolateral distribution of the ion channels and ion transporters is depicted. Figure reproduced from Stokes 1993.

A third type of IC (γ-IC), which displays both an apical and a basolateral Cl^--HCO_3^- exchanger, has been reported to exist in rabbit CCD (Emmons et al. 1994). In a sense this cell is a "hybrid" of the α-IC and ß-IC. It appears that this cell type may be the most prominent type of IC in the CCD. Although the precise function of these cells is unknown; Emmons speculated that the γ-IC could mediate HCO_3^- absorption if the basolateral Cl^- base rate exceeded the apical rate, and if an apical transport pathway for efflux of acid-equivalents is also present.

In addition, there is immunohistochemical evidence to suggest the presence of an electroneutral apical H^+-K^+-ATPase in both α-IC and ß-IC of the rabbit CCD (Wingo et al. 1990, Silver et al. 1993). However, the functional role, precise distribution and species differences of the H^+-K^+-ATPase in the CCD are not known with certainty (Schuster 1993).

1.5 Antigenic Properties of the CCD

Given the cellular heterogeneity of the CCD, investigators have sought ways to study each cell type separately in order to examine their individual properties. Monoclonal antibodies and lectins have been used extensively for this purpose.

The ß-IC can be identified by immunoreactivity of the apical and basolateral membranes with antibodies directed against H^+-ATPase or band 3 respectively; however, peanut lectin agglutinin has been used as the marker of choice for these cells in rabbit (Lehir et al. 1982, van Adelsberg et al. 1989, Schwartz et al. 1985). Peanut lectin (Arachis Hypogea) was originally found to agglutinate human red blood cells by specifically binding galactopyranosylamine residues (Lotan et al. 1975). In the rabbit CCD 80% of the IC are

peanut lectin positive and were considered to be ß-IC (Schuster et al. 1986) until recently, when a third IC subtype, the γ-IC, was also found to react with peanut lectin agglutinin (Emmons et al. 1994).

Wheat germ agglutinin has been reported to be a principal cell specific marker (Holthöfer et al. 1987, Holthöfer 1988). This lectin recognizes terminal carbohydrates of glycoproteins or glycocalix of the apical membrane of principal cells but also recognizes glomeruli.

Other monoclonal antibodies have been developed to study the evolution of PC and IC in culture (Jamous et al. 1992). The monoclonal antibody 503 (mAb 503) reacts with an antigen expressed on the apical membrane of the intercalated cells, whereas the monoclonal antibody 703 (mAb 703) was demonstrated to bind specifically to the apical membrane of CCD principal cells. The antigens recognized by these antibodies are not known with certainty. A preliminary study indicated that the antigen bound by mAb 703 is an ecto-protein sensitive to papain hydrolysis. The expression of the surface antigens labelled by these antibodies was considerably reduced with increasing length of time in culture. It is noteworthy that, many factors control the expression of surface antigens both in vivo and in culture. These factors include the type of growing surface, the physicochemical constitution of the medium, hormones and growth factors all of which may be absent or suboptimal in culture.

In addition, the technique of immunodissection developed by Smith and Garcia-Perez (1985) has led to the production of a number of PC and IC-specific antibodies. This method has had limited success in isolating collecting tubule segments from connecting

tubules which share similar surface antigens and thus crossreact with these antibodies (Bindels et al. 1991, Fejes-Tóth et al. 1987, Arend et al. 1989).

1.6.0 Modulation of CCD Structure and Function

CCD cells are capable of undergoing dramatic structural and functional changes in response to various physiologic stimuli. The functional and morphological effects of hormones, pH, ionic balance (i.e. K^+ depletion) and growth factors on CCD are particularly important to consider when developing a CCD cell culture. A careful understanding of these factors is needed in order to simulate the "*in vivo*" environment. This is relevant to my thesis which will involve the culture of CCD cells.

1.6.1 Effects of Aldosterone

The effects of aldosterone in CCD are well documented; aldosterone increases 1) the surface density of plasma membrane infoldings 2) Na^+ absorption 3) K^+ secretion and 4) Cl^- absorption (Stokes 1993). Aldosterone enhances the transport capacity by stimulating the Na^+-K^+-ATPase activity and promoting the amplification of the basolateral membrane in principal cells (Wade et al 1979, Minuth et al. 1987). Aldosterone can also increase the number of peanut lectin binding cells of cultured CCD cells (Minuth et al. 1993). Aldosterone secretion by the adrenal cortex is stimulated by angiotensin II suggesting an indirect role for the latter hormone in these processes.

Several pathophysiological conditions are also responsible for structural and functional modifications of the CCD, namely, acid/base perturbations and K^+ depletion.

1.6.2 Effects of Acid/Base Perturbations and Functional Plasticity of Intercalated Cells

During bicarbonate loading and/or during respiratory and metabolic acidosis, several investigators have observed a striking increase in apical microprojections and in the surface density of the apical membrane of α-IC in CCD (Hagège et al. 1974, Verlander et al. 1987). This suggests that the variety and intricacy of patterns of the plasma membrane observed by SEM and TEM may serve a functional purpose; to enhance cell surface area and, thus, enhance cell transport capacity.

The direction in which HCO_3^- is transported by the CCD is known to be a function of the *in vivo* acid-base status of the animal (McKinney et al. 1977). Thus, it has been suggested that ICs display functional plasticity. Schwartz and coworkers (1985) demonstrated that the HCO_3^--secreting cell can be forced to change its functional polarity to that of the H^+-secreting cell by acid-loading the animal. Others have reported considerable cellular remodelling of the apical membrane of ß-IC with endocytotic removal of the apical Cl^--HCO_3^- exchanger in response to an in vitro acid incubation (Satlin et al. 1989).

1.6.3 Effects of Potassium Depletion

K^+ depletion causes CCD tubular hypertrophy, increased activity of transport enzymes and resistance to vasopressin and aldosterone (Elger et al. 1992, Imbert-Teboul et al. 1987, Raymond et al. 1985, Mujais et al. 1992). Recent evidence that angiotensin-converting enzyme (ACE) inhibitors are able to attenuate the morphological and biochemical changes that occur in the collecting duct during K^+ depletion suggests a potential role for angiotensin II in mediating this process (Mujais et al. 1994).

CHAPTER 2

ANGIOTENSIN II

2.0 History of Angiotensin II (Ang II)

Renin, the first element of the renin-angiotensin system (RAS), was discovered by Tigerstedt and Bergmann in 1898. They found large amounts of this enzyme in kidney tissue from which it could easily be extracted. Intravenous injection of crude preparations into experimental animals produced dramatic increases in blood pressure that lasted for over an hour. Much later, Goldblatt suggested that hypertension had a humoral basis and proposed it was of renal origin. He speculated that this humoral substance was renin (Golblatt et al. 1934, 1947). Two other groups of researchers argued that renin was not a direct pressor or vasoconstrictor substance (Page et al. 1940, Braun-Menendez et al. 1940). Rather, renin acted on a substance present in plasma to produce a heat-stable, short-acting vasoconstrictor substance. Page and co-workers named the new substance "angiotonin" whereas the Braun-Menendez's group named it "hypertensin". In an effort to minimize confusion surrounding terminology both groups agreed to call it "angiotensin".

2.1 Biosynthesis of Angiotensin II and the Renin-Angiotensin System

Early in the purification of angiotensin, Skeggs et al. (1954) discovered that the substance actually exists in two different forms. Today it is well known that angiotensin II is part of a regulatory cascade, the renin-angiotensin system (RAS) initiated by renin and involving different structural forms of angiotensin.

Essentially, renin is released by the granular cells of the juxtaglomerular apparatus in response to decreases in tubular Na^+ concentration, a drop in blood pressure, or increases in sympathetic activity. Upon release, this protease cleaves a blood serum α_2

globulin, angiotensinogen, derived from hepatocytes, to yield a decapeptide, angiotensin I. Angiotensin I is converted to the octapeptide angiotensin II by a converting enzyme (ACE) a non-specific dipeptidyl carboxypeptidase present in endothelial cells and the vasculature of the lung. Angiotensin II itself is a potent vasoconstrictor and also stimulates vasopressin release. In the adrenal cortex it is converted by aminopeptidases to the hexapeptide angiotensin III, which stimulates secretion of the steroid hormone aldosterone by the adrenal cortex. This final product of the RAS is eventually degraded by angiotensinases to inactive peptide fragments (Figure 2.0).

In addition to the systemic RAS, there is well-documented evidence for the existence of local renin-angiotensin systems in several organs including adrenal, brain, heart and vasculature. The intrarenal RAS is of particular interest. All of the enzymes, substrates and receptors that make up the renin-angiotensin system are present in the kidney. Thus, locally produced Ang II may exert tonic effects within the kidney.

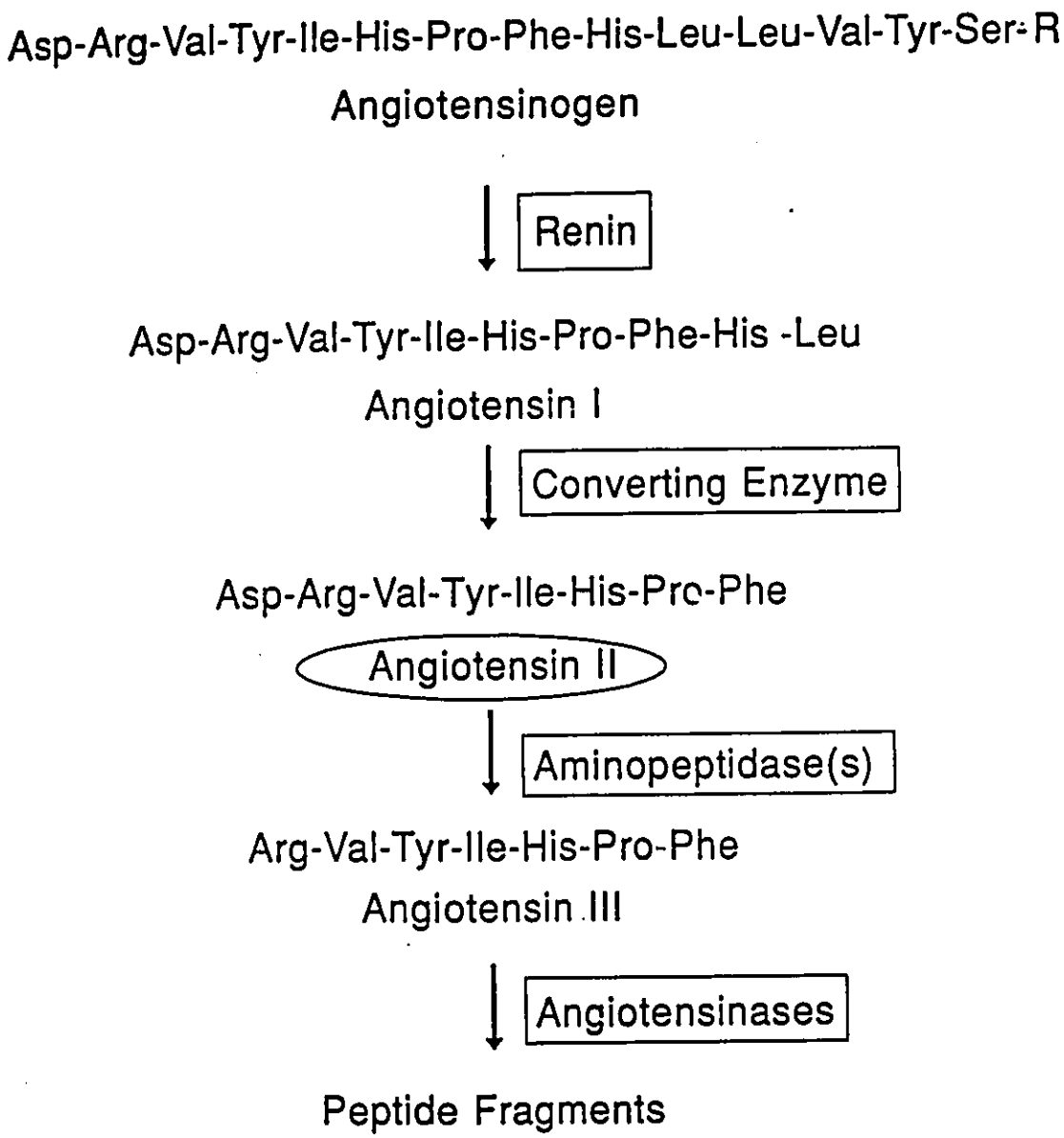

Figure 2.0

The renin-angiotensin system (RAS). The structure of Ang II and its precursors are illustrated. See text for more detail. Reproduced from Katzung 1993.

2.2 Structure and Chemistry of Angiotensin II

As noted, Ang II is an octapeptide resulting from ACE-mediated cleavage of the His-Leu carboxy-terminal residue of Ang I (figure 2.0). Ang II is metabolized during passage through most vascular beds by various angiotensinases. Although Ang II is a short-lived molecule (t½ 15-60 seconds), its effects are mediated by membrane receptors which initiate a series of signalling cascades, thus permitting sustained responses. It has a high affinity for these receptors with a K_d in the nanomolar range. The amino terminal is not essential for activity, but it does influence receptor binding and duration of action. The amino acid at position 2 (arginine) also contributes to receptor affinity, but it does not influence the intrinsic activity of the peptide. The minimum structure of angiotensin II that has full intrinsic activity is the 3-8 hexapeptide.

2.3 Angiotensin II Receptors and Signal Transduction Pathways

At least two Ang II receptor subtypes have been identified and classified according to antagonist specificity. Inhibition by Dup 753 (also known as Losartan), a biphenylimidazole, characterizes the AT_1 subtype, whereas inhibition by tetrahydroimidapyridines (PD123177, PD123319, CGP 42112A) characterizes the AT_2 subtype (Timmermans et al. 1991, 1993). The subtypes are also defined on the basis of their susceptibility to dithiothreitol, their ability to respond to angiotensin II and III and the second messenger systems to which they are coupled.

The AT_1 Ang II receptor subtypes are coupled to distinct signalling pathways that lead to the production of second messengers, which in turn direct the physiological response

of the cells. Cloning of AT_1 Ang II receptor subtypes reveals highly homologous nucleotide sequences that encode a protein of 329 amino acids, with seven hydrophobic putative transmembrane domains, consistent with a G protein-linked receptor (Burns et al. 1993). Two major signal transduction pathways have been associated with the AT_1 receptor subtype. Binding of Ang II to the AT_1 receptors induces activation of phospholipase C (PLC) with subsequent hydrolysis of inositol phosphates, increased intracellular Ca^{++} and diacylglycerol levels (Crabos et al. 1994, Burns et al. 1995). Positive coupling to phospholipases A_2 and D has also been reported (Li et al. 1994). Conversely, the second major pathway involves negative coupling to adenylate cyclase which results in decreased cAMP levels. The inhibition of adenylate cyclase activity by Ang II is mediated by a pertussis toxin-sensitive G protein (G_i) (Douglas et al. 1990). The functional effects caused by the activation of the AT_1 signalling pathways have been well documented in vascular smooth muscle cells and in proximal tubule cells. In vascular smooth muscle cells, both PLC, PLD, and PLA_2 are activated in response to angiotensin II resulting in vasoconstriction, whereas in proximal tubule cells, Na^+/H^+ exchange and Na^+/HCO_3^- cotransport are activated by angiotensin II via inhibition of adenylate cyclase (Alexander et al. 1985, Douglas et al. 1990). Although the Ang II-induced inhibition of adenylate cyclase appears to be the predominant pathway mediating Na^+ and HCO_3^- transport in proximal tubule, Ang II-mediated activation of PKC and increments in Ca^{2+} appear to play an important role as well (Wang et al. 1991, Dominguez et al. 1987).

In contrast, AT_2 receptors are not coupled to G proteins. This receptor subtype may decrease cGMP levels, due to inhibition of particulate guanylate cyclase by a

phosphotyrosine phosphatase in rat brain (Sumners et al. 1991, Bottari et al. 1992). At present, the physiological role of the AT_2 receptor remains obscure. Indeed, almost all effects of Ang II are mediated by the AT_1 receptor.

2.4 Expression and Distribution of Ang II Receptors in the Kidney

Pharmacological evidence has demonstrated a wide distribution of Ang II receptors in the kidney. Ang II receptors are present on afferent and efferent arterioles, glomerular mesangial cells, and tubular cells. More specifically, receptors for Ang II have been identified on all nephron segments with highest concentrations in the proximal tubule (Mujais et al. 1986). In the proximal tubule, these receptors appear to be localized to both the basolateral and apical membrane (Brown et al. 1982, 1983). However, not much is known about the membrane location of these receptors in other tubule segments.

The AT_2 receptor subtype is predominantly expressed in the fetal kidney suggesting that it may be involved in regulation of fetal and neonatal development (Grone et al. 1992). In contrast, *in vitro* autoradiography experiments showed that binding of Ang II was almost completely inhibited by the AT_1 receptor antagonist Dup 753 in adult kidney. Despite this, binding in the large preglomerular vessels was inhibited by the AT_2 antagonist PD123177 confirming the continued expression of the AT_2 receptor subtype in the vasculature of adult kidney (Grone et al. 1992).

2.5 Direct Tubular Effects of Renal Ang II

Independent of its effects on renal haemodynamics and glomerular filtration, Ang II can directly influence tubular function. The effects of this hormone on the function of proximal tubules has been extensively studied. In proximal tubule, Ang II stimulates the apical Na^+-H^+ exchanger (Bloch et al. 1992), increases activity of the basolateral Na^+-$3HCO_3^-$ cotransporter (Lui et al. 1989, Geibel et al. 1990), and mediates cell hypertrophy (Wolf et al. 1993, Mujais et al. 1994).

In addition, and of direct relevance to my thesis, recent studies have identified a direct role for Ang II in regulating bicarbonate reabsorption in segments distal to the proximal tubule. Ang II stimulates HCO_3^- reabsorption in the rat loop of Henle possibly via stimulation of a Na^+-H^+ exchanger (Capasso et al. 1994). Levine and coworkers demonstrated that Ang II-stimulated distal tubule bicarbonate reabsorption in rats (Levine et al. 1994).

However, the role of Ang II in modulating transport in the CCD remains incompletely understood. In this regard, a recent study in rat demonstrated a role for Ang II in regulating intercalated cell H^+-ATPase activity (Tojo et al. 1994). Furthermore, in K^+ depleted rats, hypertrophy of CCD segments is attenuated by systemic angiotensin converting enzyme inhibition, suggesting a direct effect of Ang II on CCD cell growth (Mujais et al 1994), as noted earlier.

CHAPTER 3

AIMS

3.0 Rationale

The presence of Ang II receptors in the distal nephron suggests that Ang II may play a role in CCD function. To date, there have been few studies that have examined the signalling mechanisms and functional effects of Ang II in the CCD. Precise study of hormone interaction and signalling pathways in the CCD has been technically challenging. The difficulties encountered stem from the fact that the methods employed for the isolation of CCD segments often result in low yield or contamination with other segments. A method for CCD isolation which could surmount these obstacles would be useful for the development of a permanent cell line derived from CCD.

3.1 Purpose

Thus, the purpose of this project was two fold.

First, using a novel method of CCD isolation, our objective was to immortalize a rabbit CCD cell line which retained the morphological, biochemical and physiological properties of intact CCD.

Second, to begin to characterize the role of Ang II in the CCD, we determined if AT_1 Ang II receptors were expressed by the transfected cells and studied whether well-known signalling pathways of Ang II were present in these cells.

3.2 Approach

Our laboratory in collaboration with Dr. D. Lajeunesse previously developed a new method which involves a relatively quick and simple procedure that is effective in separating enriched suspensions of collecting tubules from distal and connecting tubules (Lajeunesse et al. 1995). The method is based on the use of successive Percoll and Ficoll gradient centrifugations of collagenase-digested renal cortices (Lajeunesse et al. 1995). For my project, freshly isolated CCD segments were cultured and immortalized with a plasmid encoding the large-T antigen of SV40. Characterization of the transfected cells included: measurements of agonist-induced cAMP production, SEM, and immunohistochemistry. Ang II receptor expression was determined by radioligand-binding experiments and Northern analysis. Signal transduction pathways of Ang II were examined by measuring effects of Ang II on AVP-induced cAMP production and phosphoinositide hydrolysis.

CHAPTER 4

METHODS

4.00 General

When necessary, procedures were carried out under sterile conditions. A culture hood (Nuaire Biological safety cabinet, Plymouth, MN) was utilized to minimize contamination of solutions, isolation material, and tissue cultures. All solutions were sterilized with 0.22 μm membrane filters.

4.01 Cortical Collecting Duct (CCD) Isolation Procedure

CCD segments were isolated using a method developed in our laboratory (Lajeunesse et al. 1995). New Zealand White female rabbits of 1.5 to 2.0 kg, were maintained on a commercial diet (Purina Chow) and had free access to water. For each experiment, 2-5 rabbits were used. Rabbits were anesthetized by injection of Zylazine (10 mg/kg) and Ketamine (40 mg/kg), decapitated and bled. Kidneys were immediately removed and placed in ice-cold Krebs-Heinseleit buffer solution (KHS) consisting of (in mM): 138 NaCl, 3.9 KCl, 1.4 KH_2PO_4, 1.4 $MgSO_4 \cdot 7H_2O$, 1.2 $CaCl_2 \cdot 2H_2O$, 58 mannitol, 25 $NaHCO_3$ previously gassed with 95% O_2, 5% CO_2. Renal cortices were dissected, minced and washed extensively in ice-cold KHS supplemented with 5% bovine serum albumin (KHSB)(BSA, Intergen, New York, NY.). Minced cortices were then incubated with a gassed solution (95% O_2, 5% CO_2) of DMEM/Ham F12 (Sigma, St Louis, MO.) supplemented with 0.1% collagenase (type V, Sigma), 0.5% BSA, 51.0 mM $NaHCO_3$, 2.8 mM ascorbic acid, 10.0 mM lactic acid, 1.0 mM glutamic acid, and 1.0 mM glutamine, pH 7.4, for 20 min in a shaking water bath at 37°C. Collagenase-digested material was filtered through a 250 μm mesh brass sieve (Ingram and Bell, Don Mills, Ont.), and the filtrate collected and centrifuged

for 20 sec at 2,000 rpm, in an IEC Centra-8R swinging bucket centrifuge. The supernatant was discarded and the pellet washed and recentrifuged repeatedly with KHSB until the supernatant was clear. The tubules were resuspended in a 40% Percoll (Pharmacia, Baie d'Urfé, Qué.) solution consisting of (in mM): 138 NaCl, 3.3 KCl, 1.2 KH_2PO_4, 1.2 $MgSO_4 \cdot 7H_2O$, 0.5 $CaCl_2 \cdot 2H_2O$, 25 $NaHCO_3$, and centrifuged at 27,500 X g for 30 min at 4°C in a Sorvall centrifuge. Figure 4.01 depicts how the cells sediment in the density gradient to an equilibrium position equivalent to their own density (isopyknic sedimentation).

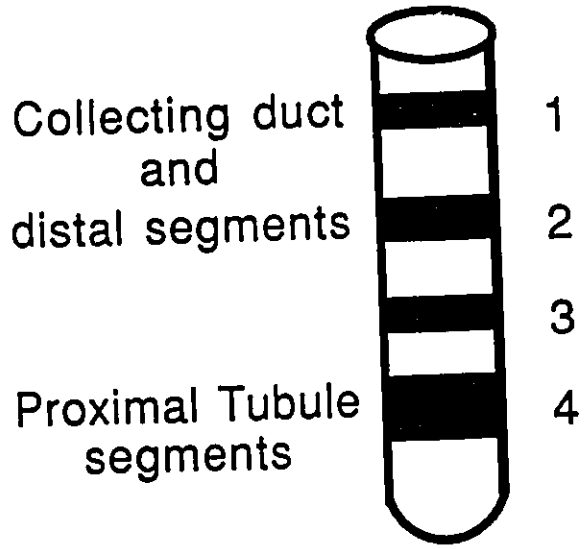

Figure 4.01

Percoll Gradient. Four bands were routinely observed. The uppermost band contained connecting and collecting tubule segments.

The uppermost band, containing distal, connecting and collecting tubule segments (Vinay et al, 1981), was recovered and washed 3 times with KHSB. The pellet was then pipetted onto a step gradient composed of 10%, 15% and 25% Ficoll (Pharmacia) in KHSB and centrifuged at 1,200 x g for 20 min at 4°C in a swinging bucket centrifuge. The band at the 10%-15% interface (B1) contained an enriched population of CCD segments as described (Lajeunesse et al. 1995) (Figure 4.02).

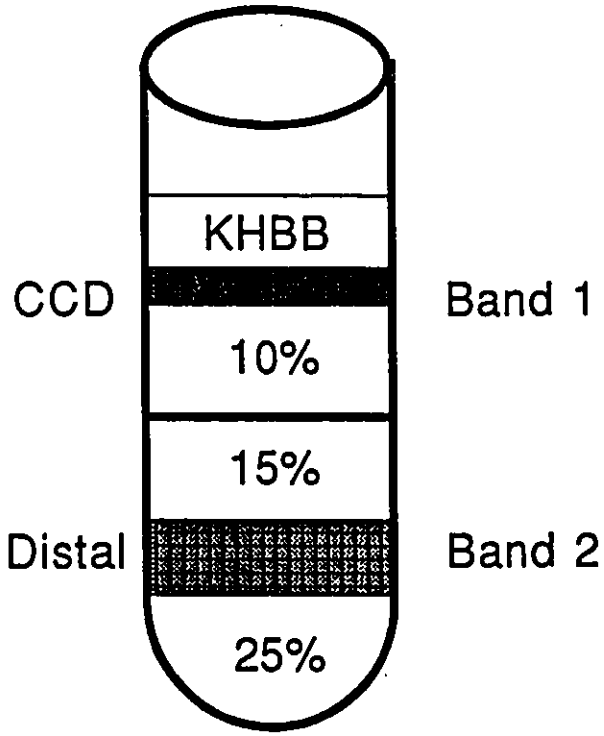

Figure 4.02

Ficoll Gradient. Band "B1" contained an enriched population of CCD cells.

4.02 Primary Culture of CCD Cells

Freshly isolated CCD segments were washed extensively in phosphate buffered saline (PBS) and plated on 100-mm tissue culture dishes in a defined media of DMEM/HamF12 initially supplemented with 10% fetal bovine serum (FBS) (Gibco, Burlington, Ont.), 600 U/ml penicillin G sodium, 600 μg/ml streptomycin sulfate (Gibco), 50 nM 17-hydroxycorticosterone (hydrocortisone) (Sigma), 2.5 nM 3, 3',5-Triiodo-L-thyronine (T_3) (Sigma), 2.5 μg/ml insulin, 2.5 μg/ml transferrin, and 2.5 ng/ml sodium selenite. The cells were grown at 37°C in a humidified atmosphere of 95% air, 5% CO_2 (CO_2/water jacketed incubator, Nuaire). After 2 days, the media was replaced and supplemented with 0.5% FBS, penicillin (100 U/ml), and streptomycin (100 μg/ml). Thereafter, media was changed every 2 days.

4.03 Immortalization of Primary CCD Cultures

The incorporation of exogenous DNA into the nuclei of cells is easily achieved by a procedure known as "transfection". Cloned DNA is often conveniently maintained as part of a bacterial plasmid. By genetic manipulation promoter sequences can be linked to a reporter gene (e.g., G-418 resistance). To induce immortalization, primary cultures of rabbit CCD cells were transfected with a plasmid (20 μg/dish) containing the large T antigen of SV40 and the gene encoding resistance to the antibiotic G-418, kindly provided by Dr. John Bell, Department of Biochemistry, University of Ottawa. The transfection was carried out utilizing the calcium phosphate precipitation method as described (Graham et al. 1973, Chen et al, 1987). Briefly, primary CCD cultures grown on 100 mm petri dishes were

incubated with a solution of 250 mM $CaCl_2$ and 40 μM chloroquine containing 20 μg of plasmid for 30 min at room temperature. Supplemented media consisting of: 90% defined media, 5% $CaCl_2$/chloroquine solution, 5% HEBS (HEBS: 50 mM Hepes, 280 mM NaCl, 10 mM KCl, 3 mM $Na_2HPO_4 \cdot 7H_2O$ pH 7.1) was then added dropwise around the perimeter of each dish and incubated at 37°C, 5% CO_2, 95% air for 6 h. At this point the cells were "shocked" with DMSO by replacing the supplemented media with defined media containing 20% dimethyl sulfoxide (DMSO, BDH) and incubating at 37°C, 5% CO_2, 95% air for 5 min. Small holes were transiently generated in the cell membrane by DMSO which allowed the DNA to enter the cell, and in some of the cells, become incorporated into the genome. The DMSO containing media was removed and cells were incubated with defined media for 48 h. Two days after transfection, culture media was aspirated and replaced with defined media containing 500 μg/ml G-418 (Gibco). Sham-transfected cells underwent the same procedure, without addition of the plasmid. After 2-3 weeks in media with G-418, no sham-transfected cells remained viable. In contrast, colonies of cells transfected with the large T antigen plasmid were visible after 2-3 weeks and were subcloned.

4.04 Subcloning

Media was aspirated and culture dishes of transfected cells were washed with Hanks Balanced Salt Solution (without Mg^{2+} or Ca^{2+}) (Gibco). Single colonies of 10-20 cells were isolated by trypsinization in a plastic ring sealed around the colonies by means of silicon grease. Trypsinized cells were aspirated with a Pasteur pipette and expanded in culture dishes containing defined media and G-418 and cultured as described in section 4.02.

4.05 Passaging of Cells

Cells were passaged when stock culture flasks (150 mm) reached confluence. Media was removed and confluent monolayers were washed with Hank's Balanced Salt solution (without Mg^{2+} or Ca^{2+}) and incubated with trypsin for 2 min at room temperature. After 2 min, the trypsin was removed and culture dishes were placed in an incubator. After 5 min, rounded cells were easily washed off plates with DMEM/HamF12. The cell suspension was centrifuged for 2 min at 2,000 rpm in an IEC Centra-8R centrifuge. The pellet was resuspended in an appropriate volume of DMEM/HamF12 to achieve the desired dilution and aliquoted onto culture dishes.

4.06 Freezing and Storage of Cells

In order to keep a stock of low passage cells, cells were routinely frozen. First, cells were trypsinized as described in section 2.05 and the pellet resuspended in DMEM/HamF12 supplemented with 10% FBS and 10% DMSO a cryo-preservative. The cell suspension was aliquoted into ice-cold cryovials, maintained at -20°C for 20 min then transferred to -70°C for 2 hours. A liquid nitrogen vessel was used to store cells until needed. Thawing of cells consisted of rapidly heating up the cryovials to 37°C and immediately plating in 5 ml culture flasks. Once cells attached to culture dishes, media containing DMSO was removed and replaced with defined media containing G-418.

4.07 Scanning Electron Microscopy (SEM)

Confluent monolayers of transfected CCD cells were grown on glass coverslips, fixed with half-strength Karnovsky's fixative (Karnovsky 1965) for 18 h then washed in 0.1 M cacodylate buffer, pH 7.4, with 0.2 M sucrose added. They were then post-fixed with 2% osmium tetroxide for 1 h, dehydrated in solutions of ethyl alcohol of increasing concentration and critical point-dried. After sputtering with platinum-palladium, cells were studied with a Philips EM 505 scanning electron microscope. Post-fixation and SEM photography was kindly performed by Vijay Kapal, Faculty of Medicine, Department of Anatomy and Neurobiology, University of Ottawa.

4.08 Immunohistochemistry

4.08.1 General

Transfected CCD cells were grown to confluence on glass coverslips, rinsed with PBS consisting of (in mM): 135.0 NaCl, 5.0 KCl, 10.0 Na_2HPO_4, 1.0 $CaCl_2 \cdot 7H_2O$, 1.0 $MgCl_2$, 5.0 glucose, pH 7.2 (Van Aldelsberg et al. 1989) and then fixed for 1 h at room temperature in 4% paraformaldehyde and 0.2% picric acid in 0.16 M sodium phosphate buffer (pH 6.9). This fixative was also used for fixation of wedge slices of rabbit kidney. Slices were frozen in dry ice and sectioned 14 μm thick with a Zeiss cryostat.

Primary antibodies were applied to fixed monolayers or tissue sections in PBS containing 0.3% Triton X-100 for 18 h at 4°C. Slides were washed extensively with PBS before application of secondary antibodies. Negative controls underwent the same procedure with omission of the primary or secondary antibody.

Anti-fade mounting medium consisting of PBS containing 0.1 mM phenylaminediamine and 10% glycerol was applied to the monolayers prior to sealing with coverslips. All slides were examined with a Zeiss Axioplan microscope. Photographs were taken with Kodak Tri-X black and white film or Kodak ektachrome color slide film. Random fields of immunolabelled cells were photographed and the number of labelled cells determined using a computer image analysis program (MacIntosh Image 1.47 software).

4.08.2 Large T Antigen

In order to determine the efficiency of transfection, cells were prepared as described above and incubated with mouse hybridoma antibodies (American Type Culture Collection (ATCC), Rockville, MD) specific for the large T antigen of SV40 (1:2 dilution). For visualization, the cells were incubated with a secondary biotinylated sheep anti-mouse antibody (Amersham, Oakville, Ont.), diluted 1:50, for 4 h at 37°C, followed by streptavidin-labelled texas red, diluted 1:100 in PBS (Amersham) for 2 h at room temperature.

4.08.3 mAb 503 and mAb 703

The identification of principal and intercalated cells was performed with monoclonal antibodies kindly provided by Dr. Philippe Poujeol, Département de Biologie cellulaire et moléculaire, CEN Saclay, France. mAb 703 binds to the apical membrane of principal cells whereas mAb 503 binds to the apical membrane of intercalated cells (Tauc et al. 1992). The antibodies were applied in a 1:1 dilution in PBS. For visualization, secondary FITC-

labelled sheep anti-mouse antibodies, diluted 1:20 (Amersham) were applied for 35 min at 37°C.

4.08.4 Peanut Lectin Agglutinin

The binding of Peanut Lectin Agglutinin (PNA) (*Arachis Hypogea*, Intermedico, Markham, Ont) was performed on confluent monolayers of cells grown on coverslips, washed with PBS, and incubated with fluorescein isothiocyanate-labelled peanut lectin (50 μg/ml) in PBS for 10 min at room temperature, followed by fixation.

4.09 Histochemistry for Alkaline Phosphatase

Cells were grown to confluence and assayed for alkaline phosphatase activity, by the method of McGadey (1970). Cells were washed with a Tris-HCl buffer (100 mM Tris HCl, 100 mM NaCl, 50 mM $MgCl_2$, pH 9.5) and incubated with 4-nitro-blue-tetrazolium chloride (NBT 0.33 mg/ml) and 5-bromo-4-chloro-3-indolyl-phosphate-4-toluisin salt (BCIP 0.165 mg/ml). Incubation was carried out for 24 hours at 37°C at which time, color development was assessed. Primary cultures of proximal tubule cells, prepared as previously described (Harris 1992), were used as positive controls.

4.10 Measurement of Cyclic Adenosine Monophosphate (cAMP)

Hormone-induced cAMP responses were assayed in transfected CCD cells. Cells were grown to confluence in 24-well plates and preincubated with DMEM/HamF12 containing 0.5 mM isobutyl-methyl xanthine (IBMX, Sigma) and 0.1% BSA for 15 min at

room temperature. IBMX is a phosphodiesterase inhibitor which inhibits the breakdown of cAMP to 5'AMP (Beavo, 1970). Agonists were then added for 10 min at room temperature. The reaction was stopped by removing media and adding ice-cold 10% trichloroacetic acid (TCA, v/v). Samples were repeatedly extracted with water-saturated diethyl-ether and adjusted to pH 7.0 with Tris. cAMP was assayed by radioligand binding (cAMP assay kit, Intermedico).

The cAMP assay is based on the work of Gilman (1970) and utilizes the principle of competitive protein binding in which unlabelled cAMP and a fixed amount of [^{3}H]-cAMP competitively bind a protein (cAMP dependent protein kinase) which has high specificity and affinity for cAMP. The amount of labelled protein-cyclic AMP complex formed is inversely proportional to the amount of cyclic AMP present in the assay sample. The free [^{3}H]-cAMP is removed by adsorption onto coated charcoal followed by centrifugation. An aliquot of the supernatant is removed for liquid scintillation counting which measures the protein bound [^{3}H]-cAMP. A linear standard curve is then used to determine the concentration of unlabelled cAMP in unknowns (Figure 4.03). The following mathematically derived linear equation was used to calculate cAMP concentration:

$$\% \text{ bound} = a \cdot \text{Log}[x] + b$$

where "% bound" is cpm unknown/ cpm maximal binding x 100, "a" is the slope, "b" is the y ordinate (a and b can be determined by linear regression), "[x]" is the concentration of cAMP of the sample (unknown). Solving for [x]:

$$[x] = 10^{\frac{(\% \text{ bound} - b)}{a}}$$

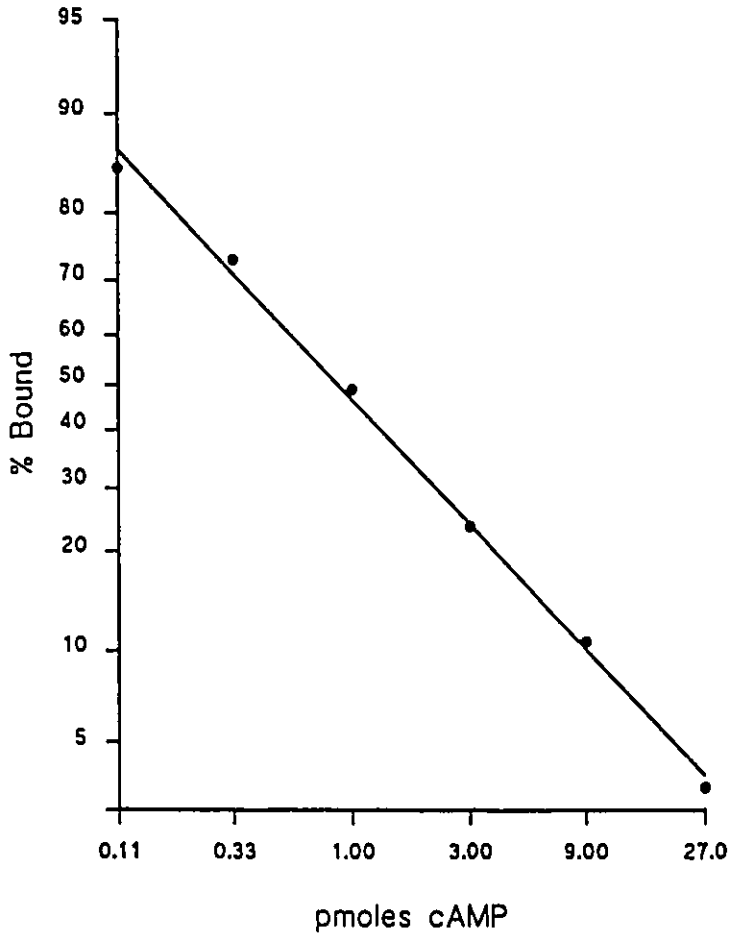

Figure 4.03

cAMP standard curve. Unlabelled cAMP standards of known concentrations were incubated with a fixed amount of [^{3}H]-cAMP and a fixed amount of binding protein. The maximal binding capacity of the binding protein was determined by incubating the binding protein with excess [^{3}H]-cAMP in the absence of unlabelled cAMP. % Binding was defined as: (cpm of standard / cpm of max binding) x 100. % Binding of standards was plotted vs log of the standard concentration (pmoles cAMP/100µl). The slope and ordinate were determined by linear regression thus permitting the determination of cAMP content of unknowns by mathematical derivation (equation in text). Data shown is that of a representative standard curve.

4.11 Assay of Phosphoinositide Hydrolysis

Phosphoinositide turnover, the breakdown of phosphatidylinositol-4,5-bisphosphate (PIP_2) to inositol phosphates (IP_1, IP_2, IP_3), in response to various agonists was measured by anion exchange column chromatography as described (Dean et al. 1989). Cells were grown to confluence in 6 well-plates, washed 3 times with inositol-free RPMI media and incubated with 3 μCi/ml [^{3}H]-myo-inositol (Amersham) in inositol-free RPMI media for 72 h. Cells were washed four times then incubated with Hank's Balanced Salt Solution containing 10 mM LiCl for 15 min at room temperature. LiCl inhibits the IP_1 phosphatase which causes the breakdown of IP_1 to inositol (Berridge 1993). This was followed by incubation with agonists in the same medium for 15 min at room temperature. Reactions were terminated by addition of ice-cold 10% TCA (v/v). Samples were extracted four times with water-saturated diethyl-ether, and brought to pH 7.0 with Tris. Columns were prepared by dissolving 0.5 g of AG 1-X8 anion exchange resin (Bio- Rad, Mississauga, Ont.) in 1 ml H_2O and pipetting the slurry into each column. 4 ml of a solution consisting of 5 mM Borax and 0.5 mM EDTA was added to equilibrate the columns prior to the addition of the samples. The inositol phosphates were successively eluted with solutions of increasing anionic strength (IP_1: 20ml of 0.2 M NH_4formate + 0.1 M formic acid, IP_2: 20ml of 0.4 M NH_4formate + 0.1 M formic acid, and IP_3: 20ml of 0.8 M NH_4formate + 0.1 M formic acid). 3 ml of each eluate solution was removed for scintillation counting.

4.12 ^{125}I-Ang II Binding Assay

Binding of ^{125}I-Ang II was performed as described previously (Burns and Harris 1995). Confluent cell monolayers in 24-well dishes were washed 2 times with PBS containing 0.5% albumin, and incubated with ^{125}I-Ang II (0.05 - 8.0 nM, specific activity 0.022 μCi/μl, Amersham) in PBS containing 0.5% BSA for 1 hour at room temperature. Nonspecific binding was determined by incubating cells with an excess of unlabelled Ang II (1 μM). After 1 hour, cells were washed 4 times with ice-cold PBS containing 0.5% albumin. Cells were solubilized with 1 N NaOH and radioactivity counted in a gamma counter.

4.13 Northern Analysis

4.13.1 RNA Isolation

Total RNA was isolated by the acid guanidinium isothiocyanate-phenol-chloroform method (Chomczynski et al. 1987). This method was selected because of its simplicity and because guanidinium thiocyanate is one of the most effective protein denaturants and inhibitors of ribonucleases (Gordon 1972) thus permitting good recovery of RNA.

Confluent monolayers grown on 100 mm culture dishes were washed twice with PBS prior to addition of 3 ml of a denaturing solution consisting of: 4 M guanidinium thiocyanate (Sigma), 25 mM sodium citrate (Sigma), pH 7.0; 0.5% lauryl sarcosine (Sigma), 0.1 M 2-mercaptoethanol (Sigma). The gelatinous lysate was scraped off the culture dishes, poured into sterile 50 ml centrifuge tubes and homogenized with a hand held homogenizer (3 x 5 sec bursts) then aspirated with a 20" syringe needle to shear DNA. Homogenates

were centrifuged at 10,000 x g for 15 min a Sorvall centrifuge. The pellets were discarded and the supernatant transferred to fresh sterile 50 ml centrifuge tubes and mixed with 0.1 ml (v/ml) 2M sodium acetate (pH 4.0), 1.0 ml (v/ml) water saturated phenol, 0.2 ml (v/ml) chloroform: isoamyl alcohol (49:1). The entire mixture was vigorously shaken, cooled on ice for 10 min and centrifuged at 5,000 x g for 10 min at 4°C. The RNA, contained in the upper aqueous phase, was transferred into a sterile 50 ml centrifuge tube containing 1 volume of phenol: chloroform (1:1), vortexed vigorously and centrifuged at 5,000 x g for 5 min at 4°C. To precipitate the RNA, the supernatant of the preceding step was vortexed with 1 volume of isopropanol at room temperature for 30 min then centrifuged at 10 000 x g for 30 min at 4°C. The glassy white pellet was resuspended in: TE (400 µl), 3 M sodium acetate (40 µl) and 2.5 volumes of 100% ethanol, kept at -70°C for 15 min, then centrifuged 10,000 x g for 15 min at 4°C. Finally, the pellet of RNA was reconstituted with 0.1% diethyl pyrocarbonate (DEPC, BDH) treated water and the O.D 260/280 measured with a spectrophotometer (Beckman Du-65, Missassauga, Ont.) to verify the purity and the final concentration.

4.13.2 Poly(A)$^+$ RNA Purification

The majority of mRNAs of mammalian cells carry tracts of poly(A)$^+$ at their 3' termini and can be separated from the bulk of cellular RNA (tRNA and rRNA) by affinity chromatography on oligo(dT)-cellulose (Edmonds et al. 1971; Aviv et al. 1972). The nonpoly(A)$^+$ species are not bound and are readily washed off the column. The bound poly(A)$^+$ RNA is eluted by lowering the amount of salt in the column buffer.

A slurry was prepared by suspending 0.025 g oligo(dT) (Sigma) in a loading buffer A: 20 mM Tris (pH 7.4), 0.1 M NaCl, 1.0 mM EDTA, 0.1 % SDS and 0.02 N NaOH. The oligo(dT) cellulose slurry was poured into a sterile disposable plastic column and washed with a solution of 0.1 N NaOH and 5 mM EDTA and then with H_2O until pH of effluent was less than 8. Loading buffer B consisting of: 40 mM Tris (pH 7.4), 1.0 M NaCl 1.0 mM EDTA, was added to equilibrate the column. Samples of total RNA (1-10 mg) were resuspended in 500 µl sterile H_2O, heated to 65°C for 5 min, mixed with 500 µL of loading buffer B and cooled to room temperature for 2 min. Heating the RNA is necessary to disrupt regions of secondary structure that might involve the poly(A)$^+$ tail. This 1.0 mL sample was added to the column, the eluate collected, and once again heated to 65°C for 5 min, cooled for 2 min and reapplied to the column. The column was then washed with loading buffer A to elute the nonpoly(A)$^+$ RNA. Finally, the poly(A)$^+$ RNA was eluted with a buffer consisting of: 10.0 mM Tris (pH 7.4), 1.0 mM EDTA and 0.05% SDS. The eluate was collected and the O.D. 260/280 was measured with a spectrophotometer (Beckman).

4.13.3 Electrophoresis of RNA on Agarose/Formaldehyde Gels.

This method is an adaptation of methods described by Miller 1987, and Lehrach et al. 1977. Essentially, mRNA samples were prepared in a gel sample buffer consisting of: 1X MOPS (10X= 0.2 M 3-(N-morpholino) propanesulfonic acid (MOPS), 50 mM Na acetate, 10 mM EDTA, pH 7.0), 17% formaldehyde, 50% formamide and 10% FLB (FLB= 1 mM EDTA pH 8.0, glycerol 50%, 0.25% bromophenol blue, 0.25% xylene cyanole).

Ethidium bromide (1-2μg/ml) was added for visualization of selected samples. Samples were heated to 65°C for 15 min in a heating block to denature, then immediately chilled on ice prior to loading onto gel. Samples were loaded onto denaturing 1% agarose/2.2 M formaldehyde gels in 20 mM MOPS. The gel was run at 5-6 volt/cm for 2-3 hours, photographed, washed extensively in double distilled H_2O to remove formaldehyde and soaked in 10 X SSC (1 X SSC consists of: 1.5 M NaCl, 0.15 M sodium citrate, pH 7.0) prior to blotting.

4.13.4 Northern Blotting

The gel mRNA was transferred by capillary blotting in 10 X SSC (1 X SSC = 1.5 M NaCl, 0.15 M sodium citrate, pH 7.0) to nylon membranes (Schleicher and Schuell, Keene, NH) overnight, as described by Reed et al. 1985. RNA was fixed to membranes by ultraviolet crosslinking (Bio Rad UV crosslinker) which involves the formation of cross-links between a small fraction of the bases in the RNA and the positively charged amine groups on the surface of the membrane (Khandjian 1987, Church et al. 1984).

4.13.5 Preparation of Radioactive Probes

It has been known for many years that oligonucleotides can serve as primers for initiation of DNA synthesis on single-stranded templates by DNA polymerases (Goulian 1969). In order to prepare radioactive probes, a random priming method for cDNA labelling was performed using a multiprime DNA labelling kit. 50 ng (5 μL) cDNA of the rabbit AT_1 Ang II receptor and 21 μL of ddH_2O were heated in boiling water for 5 min and

immediately placed on ice. The denatured cDNA is incubated with buffer, primer, [^{32}P]-dCTP (0.22 μCi/ μL specific activity), and the Klenow fragment of E. coli DNA polymerase I for 1 h at 37°C. Free nucleotides were separated from probe by centrifugation through a small column of Sephadex G-50 (Boehringer Mannheim). A 1 μL aliquot of probe was counted by scintillation spectrometry, and if radioactivity measured was greater than 0.2-1 x 10^9 cpm/μg DNA the probe was used for Northern hybridization.

4.13.6 Northern Hybridization

The method used is a modification of the method described by Southern (1975). Blots (nylon membranes) were probed with a ^{32}P-labelled cDNA probe (0.2-1 x 10^9 cpm/μg) representing the full-length open reading frame of the rabbit AT_1 Ang II receptor, in a hybridization solution consisting of 30% formamide, 0.1% sodium dodecyl sulfate (SDS), 50 mM NaH_2PO_4, pH 7.0, 5 X Denhardt's solution (0.1% BSA, Ficoll, and polyvinylpyrrolidine), 100 μg/ml salmon sperm DNA, 5 x SSC, and 10% dextran sulfate. Hybridization was performed overnight at 42°C. The membranes were washed under high stringency conditions in 2 x SSC, 0.1% SDS for 15 min at room temperature, followed by 0.2 x SSC, 0.1% SDS at 65° for 45 min and exposed overnight at -70°C to Kodak X-Omat AR film with intensifying screen.

4.14 Protein Determination

Protein content was determined using a modified Lowry method (Markwell et al. 1978). Monolayers were incubated with 1 N NaOH overnight at 37°C to dissolve protein. An aliquot of protein sample was diluted with ddH_2O and mixed with Reagent A (2.5% SDS, 2.5% Na_2CO_3, 0.025% $CuSO_4$, 0.05% Potassium Tartrate and 0.2N NaOH) for 10 min. Reagent B (1.7% Folin Ciocalteau reagent in ddH_2O) was added to samples and color development was measured at 750 nM with a Beckman DU-65 spectrophotometer. A BSA standard curve was constructed and protein concentration of samples was determined from this curve (Figure 4.04).

4.15 Statistics

Results are expressed as means ± SEM. To determine statistical significance, Student's t-test with the Bonferroni correction or analysis of variance (ANOVA) was performed. Significance considered as $p < 0.05$. A Prism graph analysis program for sigmoidal dose response curves was used to determine the EC_{50} of AVP and PGE_2.

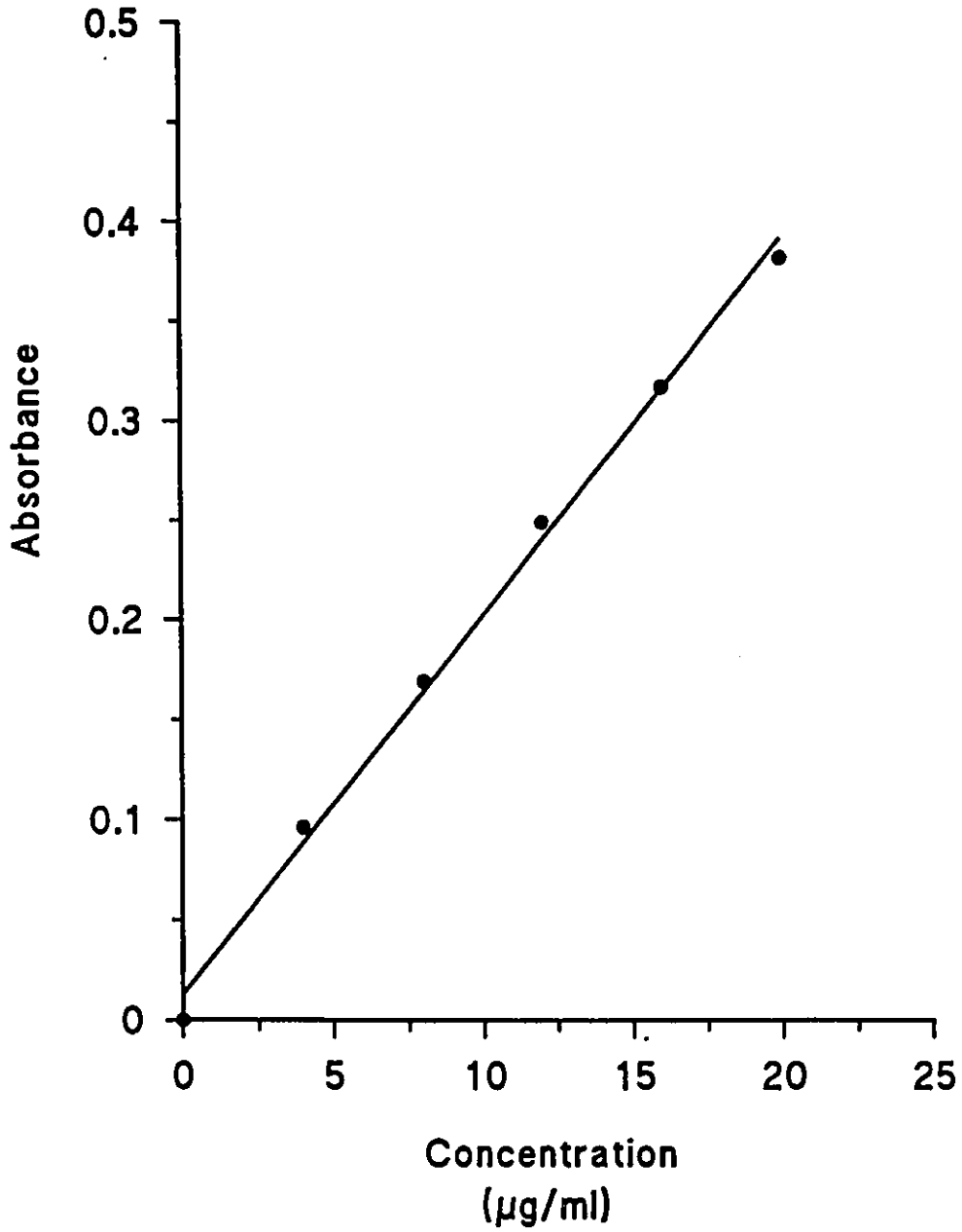

Figure 4.04

Protein standard curve. The absorbance of BSA standards of known concentration was measured at a wavelength of 750 nM with a Beckman Du-65 Spectrophotometer. Absorbance of standards was plotted against protein concentration (µg/mL). Using a Quant II Linear Soft-Pac module, the protein content of unknowns were determined. Data shown is that of a representative standard curve.

CHAPTER 5

RESULTS

Part I

Hormonal, Morphological and Antigenic Characterization of Transfected CCD Cells

5.0 cAMP responses

Fresh CCD segments were obtained by collagenase digestion of rabbit kidney cortices, followed by successive Percoll and Ficoll centrifugations as described (Lajeunesse et al. 1995) and then plated for primary culture. To induce immortalization, the primary cultures were transfected with a plasmid encoding the large T antigen of SV40, and colonies selected by resistance to G-418, as described in methods. A number of clones were obtained and screened for cAMP responses to agonist stimulation. Figure 5.00 illustrates results obtained with a single clone of transfected cells selected for study, in which cAMP responses were characteristic of rabbit cortical collecting duct (Morel et al. 1976). In this clone, both AVP (10^{-7}M) and PGE_2 (10^{-7}M) increased cAMP levels (control: 4.1 ± 0.4, AVP: 128.0 ± 17.0*, PGE_2: 12.9 ± 2.1 pmol/mg protein; * $p<0.001$, n=4-5). However, the increase observed with PGE_2 was not statistically significant by ANOVA. In contrast, salmon calcitonin (sCT) (10^{-7}M) or parathyroid hormone (PTH) (10^{-7}M) had no effect on cAMP production (sCT: 5.0 ± 1.7 and PTH: 3.9 ± 0.9 pmol/mg protein; p=NS, n=5).

sCT and PTH stimulate the production of cAMP in distal and connecting tubule cells (Charbadès et al. 1975, 1976). Therefore, the lack of a stimulatory effect on cAMP in this cell clone suggested that contamination with distal tubule and connecting duct cells was not significant.

5.1 Dose Response Curves for AVP and PGE_2

AVP and PGE_2 dose-dependent cAMP production was measured in transfected CCD cells (Figure 5.01). The EC_{50} for AVP was 6.2 nM and the EC_{50} for PGE_2 was 169.4 nM. Both curves have a sigmoidal shape, typical of a V_2 receptor and EP_2 receptor subtype mediated responses (Imbert et al. 1975, Noland et al. 1993). The threshold response occurred at about 10^{-10}M and 10^{-9}M for AVP and PGE_2 respectively, and the maximal response at 10^{-5}M for AVP (maximal response for PGE_2 undetermined).

The rabbit CCD is one of few tissues known to express all of the PGE_2 receptor subtypes. Therefore, in order to further characterize the transfected CCD cells I began to examine whether they expressed any or all of these receptor subtypes. Although statistics were not performed on dose response curves obtained with PGE_2 analogues (because of insufficient number of observations (n=2)), it does appear that butaprost, an EP_2 receptor subtype analogue, also caused dose dependent increases in cAMP levels (n=2) (table 5.0). As expected, sulprostone, an EP_3 selective PGE_2 receptor subtype analogue, did not increase cAMP levels (n=2) (table 5.1). Of particular interest, PGE_2 was unable to inhibit AVP-stimulated cAMP production, an EP_3 receptor-mediated event. Conversely, when PGE_2 (10^{-5}M, 10^{-6}M) and AVP (10^{-8}M) were incubated together, a significant increase in cAMP levels from AVP levels alone was observed (n=3, $p<0.05$) (table 5.2). The reader is reminded that these results are preliminary and the subject of ongoing research in our laboratory.

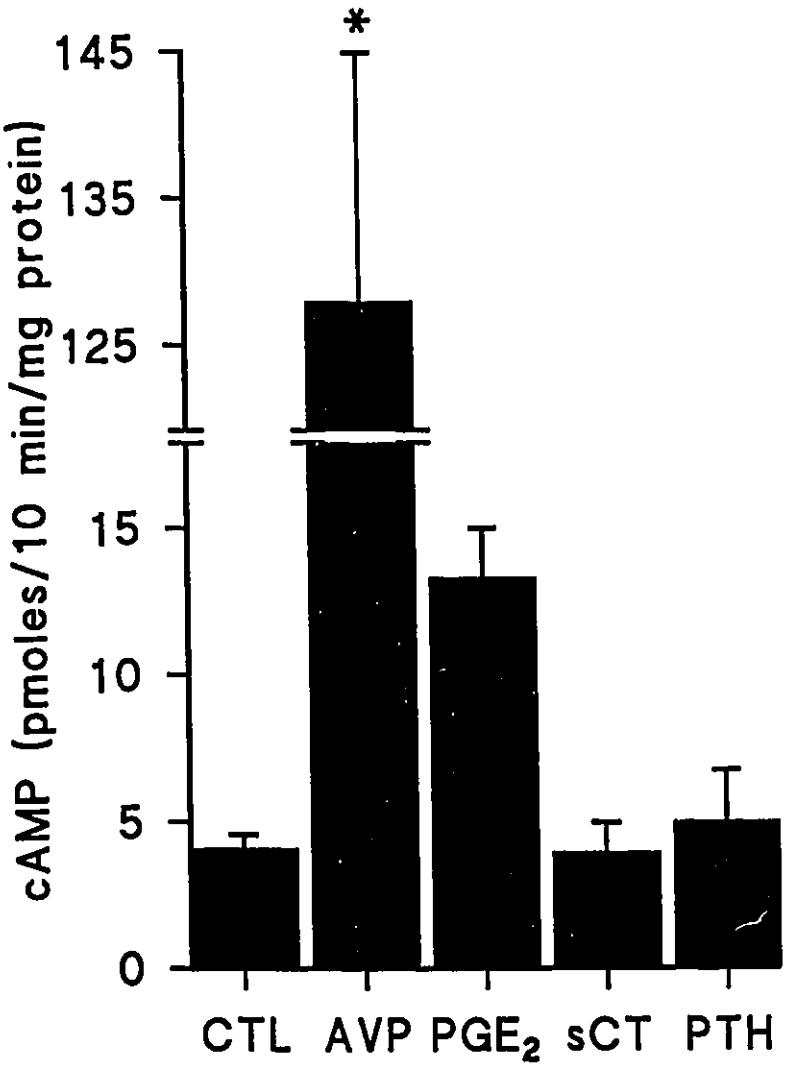

Figure 5.00

Effect of hormones on cAMP production in transfected CCD cells. Cells were incubated with arginine vasopressin (AVP), prostaglandin E_2 (PGE_2), salmon calcitonin (sCT), or parathyroid hormone (PTH) all [10^{-7}M] or vehicle (CTL). cAMP levels were determined by radioimmunoassay (RIA). Results are means ± SEM of 5 or 4 experiments done in duplicate *$p<0.001$ vs control.

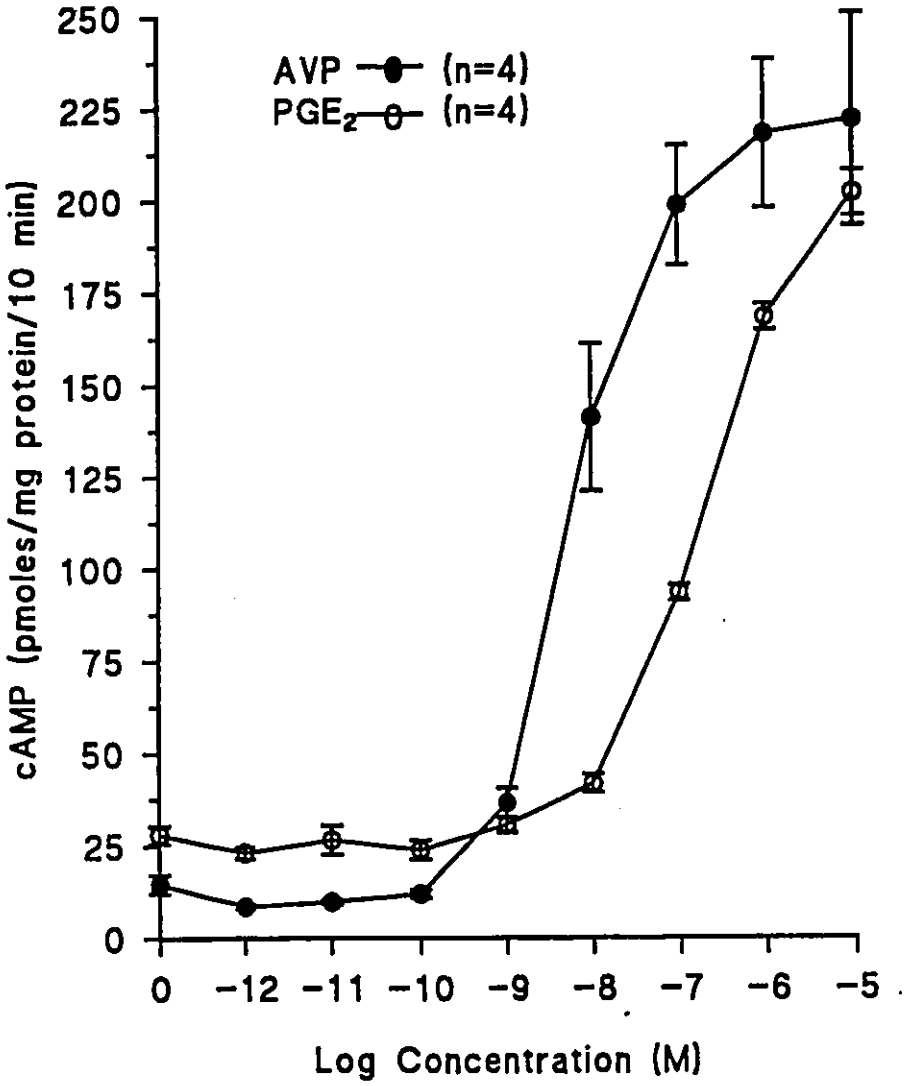

Figure 5.01

cAMP accumulation in response to AVP and PGE_2 in transfected CCD cells. AVP and PGE_2 concentrations are plotted in abscissa. In ordinate, cAMP production is expressed in picomoles cAMP produced per mg protein per 10 min incubation. Each point is the mean value of 4 experiments done in duplicate ± SEM.

Table 5.0

Dose Dependent Effect of Butaprost on cAMP Levels cAMP pmoles/mg protein/10 min		
Concentration (M)	**Mean (n=2)**	**SD**
Control	63.22	7.8
10^{-10}	46.41	5.8
10^{-9}	47.20	4.0
10^{-8}	67.33	6.8
10^{-7}	131.94	20.4
10^{-6}	258.45	7.2
10^{-5}	335.92	70.0

Table 5.1

Dose Dependent Effect of Sulprostone on cAMP Levels cAMP pmoles/mg protein/10 min		
Concentration (M)	**Mean (n=2)**	**SD**
Control	11.73	4.4
10^{-12}	7.87	2.5
10^{-11}	6.99	1.2
10^{-10}	10.20	2.1
10^{-9}	9.45	0.7
10^{-8}	10.81	1.6
10^{-7}	10.43	2.6
10^{-6}	10.50	0.4
10^{-5}	11.01	0.9

Table 5.2

cAMP Production in Transfected CCD Cells pmoles/mg protein/10 min		
Agonist Concentration (M)	**Mean (n=3)**	**SEM**
Basal	17.00	6.20
AVP (10^{-8}M)	86.19	15.00
AVP (10^{-8}M) + PGE_2 (10^{-5}M)	228.30	37.53 *
AVP (10^{-8}M) + PGE_2 (10^{-6}M)	197.94	24.50 *
AVP (10^{-8}M) + PGE_2 (10^{-7}M)	138.25	15.39
AVP (10^{-8}M) + PGE_2 (10^{-8}M)	89.47	10.89
AVP (10^{-8}M) + PGE_2 (10^{-9}M)	80.75	16.34
AVP (10^{-8}M) + PGE_2 (10^{-10}M)	71.20	18.38
AVP (10^{-8}M) + PGE_2 (10^{-11}M)	69.22	13.28
AVP (10^{-8}M) + PGE_2 (10^{-12}M)	80.60	11.12

Cells were preincubated with AVP for 10 min prior to incubation with AVP + PGE_2. The half maximal dose (EC_{50}) for AVP (10^{-8}M) was selected arbitrarily to determine if various concentrations of PGE_2 were capable of inhibiting AVP-stimulated cAMP accumulation. * $p < 0.05$ vs AVP (10^{-8}M) alone.

5.2 Phase Contrast Micrograph of Transfected CCD Cells

In order to examine the appearance of monolayers of transfected CCD cells, low magnification phase contrast micrographs were taken of cells grown on glass coverslips (Figure 5.02). The cells appeared to form a single monolayer. The outline of the individual cells, although not always clearly visible, appeared to be polygonal. However, certain cells displayed a more rounded shape with a larger surface areas than those of the polygonal cells. The monolayer appeared to be of an epithelial nature in that epithelial cells have a characteristic regular, polygonal shape with a clearly defined edge in culture, unlike fibroblasts which display a fibrous appearance, or smooth muscle cells which have an elongated star-like appearance (Freshney 1994). Furthermore, confluent monolayers sometimes displayed hemicyst-like "domes", a marker of polarized transporting epithelia (Rabito et al. 1980, Tanner et al. 1984).

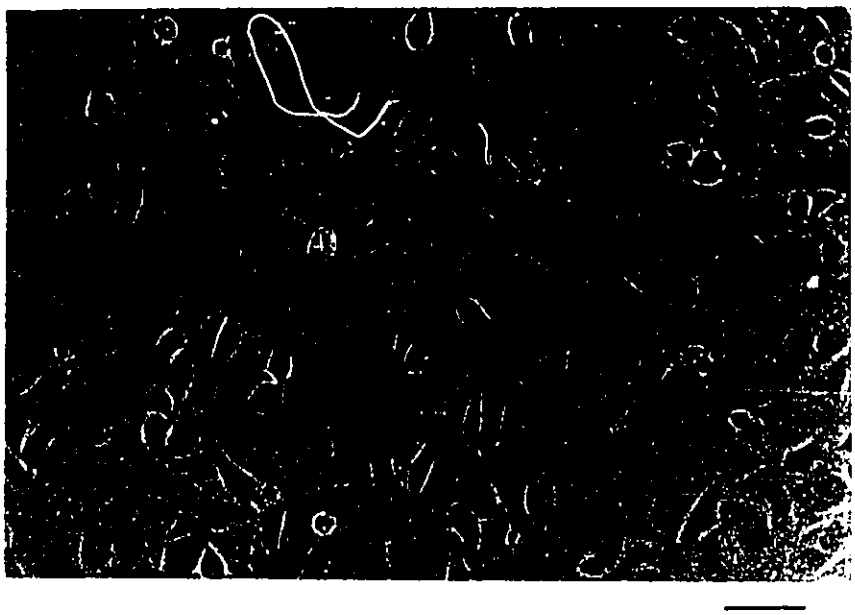

Figure 5.02

Phase contrast micrograph of transfected CCD cells. Transfected CCD cells were grown on coverslips and fixed. Photomicrographs were taken at low magnification in order to view the appearance of the cell monolayer. Scale bar 50 μm.

5.3 Expression of Large T Antigen

To determine if transfected cells in this clone expressed the large T antigen, cells were grown on coverslips, fixed and incubated with polyclonal antibodies specific for the large T antigen of SV40 (Figure 5.03). This experiment was performed twice on cells of passage 3 and 8 and both times the immunoreactivity, localized to nuclei, was detected in 100% of the cells. In addition, a double labelling experiment was performed using the large T antigen antibodies and Hoerscht reagent. Hoechst reagent labels double stranded nuclear DNA (Labarca et al. 1980). In transfected CCD cells, all nuclei labelled with Hoechst also labelled with the large T antigen (not shown). MDCK cells, used as negative controls, displayed no fluorescence (results not shown). Negative controls consisting of omission of primary or secondary antibody displayed no fluorescence (results not shown).

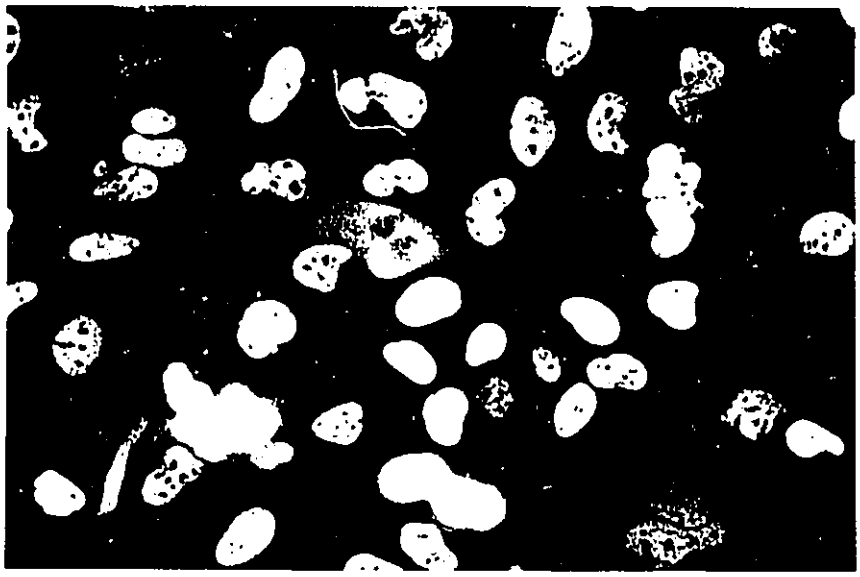

Figure 5.03

Identification of nuclear SV40 large T antigen in transfected CCD cells. Cells were grown on coverslips, fixed, and incubated with hybridoma mouse antibodies specific for SV40 large T antigen. The nuclear stain confirms that 100% of transfected cells were positive for the large T antigen. Scale bar: 50 μm.

5.4 Scanning Electron Microscopy (SEM)

SEM was performed to determine if the transfected CCD cells also retained the morphological features of CCD. The distinguishing feature of α-IC is a microplicated (pleated) surface (Verlander et al. 1987, Evan et al. 1991). Microplicae are microfolds of the apical membrane which give the cell a sponge-like appearance (Hagège et al. 1974). In contrast, PC and ß-IC display short stubby microvilli sparsely distributed over the entire surface (Lefurgey et al. 1979, Kaissling et al. 1982). At 20,000 X magnification, cells displayed one of two morphological appearances (Figure 5.04) 1) a microplicated apical surface, as described for α-IC or 2) a smoother surface with few microvilli. In *situ*, PC display a single central cilium on the apical surface (Lefurgey et al. 1979). This feature was not observed on any of the transfected cells grown on glass coverslips.

Figure 5.04

SEM of transfected CCD cells. Two different cell surface morphologies resembling those of PC and IC are displayed. Microplicae, suggestive of α intercalated cells (IC) are shown at higher magnification (20,000 X) in the upper left inset. Principal cell (PC) and ß-IC typically display only a few sparsely distributed microvilli as shown at higher magnification (20,000 X) in the bottom left inset. Magnification 8,000 X.

5.5 Immunofluorescence

Since SEM studies could not distinguish PC from ß-IC, further studies were performed utilizing immunofluorescent labelling of cells with either mAb 703, a PC antibody, or mAb 503, an IC antibody (Tauc et al. 1992). As shown in Figure 5.05 and Figure 5.06, distinct populations of cells were identified with each of these antibodies. 9.6 ± 2 % (n=10 fields) of cells reacted with the PC antibody, while 16.2 ± 6 % (n=10 fields) were labelled with the IC antibody. Note that the 10 fields were obtained from 4 separate slides and that the total number of cells observed was ~ 1000. For both antibodies, the intensity of immunofluorescence was variable. Some cells were intensely labelled, while others demonstrated weaker fluorescence. In both instances, the labelled cells were mainly in clusters of 5-10 cells. However, a few sparsely distributed fluorescent cells were seen intermingled with non-fluorescent cells. The specificity of mAb 703 (figure 5.07) and mAb 503 (figure 5.08) was demonstrated in sections of rabbit kidney. Negative controls consisting of omission of primary or secondary antibodies yielded no fluorescence (not shown).

Since rabbit CCD also contains ß-IC, the binding of peanut lectin agglutinin, which has been shown to specifically bind to terminal D-galactosyl residues on the apical membrane ß-IC (LeHir et al. 1982), was determined. As shown in Figure 5.09, peanut lectin-positive cells (26.6 ± 5 %, n=10 fields of 4 slides) were easily identifiable, although variable intensities of fluorescence were observed. Peanut lectin binding was completely inhibited by incubation of cells with 300 mM galactose (not shown). The specificity of peanut lectin was demonstrated in rabbit kidney sections (Figure 5.10).

These results suggested that PC, α-IC or ß-IC, were present in our immortalized cell

line. In order to determine the total % of cells identifiable by these markers, transfected cells were incubated with all three of peanut lectin agglutinin, mAb 503, and mAb 703. This was achieved in three stages, as illustrated in Figure 5.09. As noted, Figure 5.09 A shows the binding of FITC-labelled peanut lectin agglutinin to cells; Figure 5.09 B depicts immunofluorescence of mAb 503 and mAb 703 labelled with biotin and streptavidin-texas red in the same field. Figure 5.09 C is the corresponding double-labelled immunofluorescent micrograph utilizing all three agents. Greater than 50% of cells were labelled with one or more of these agents. Occasional cells were observed which labelled with both peanut lectin agglutinin and either mAb 503 or mAb 703.

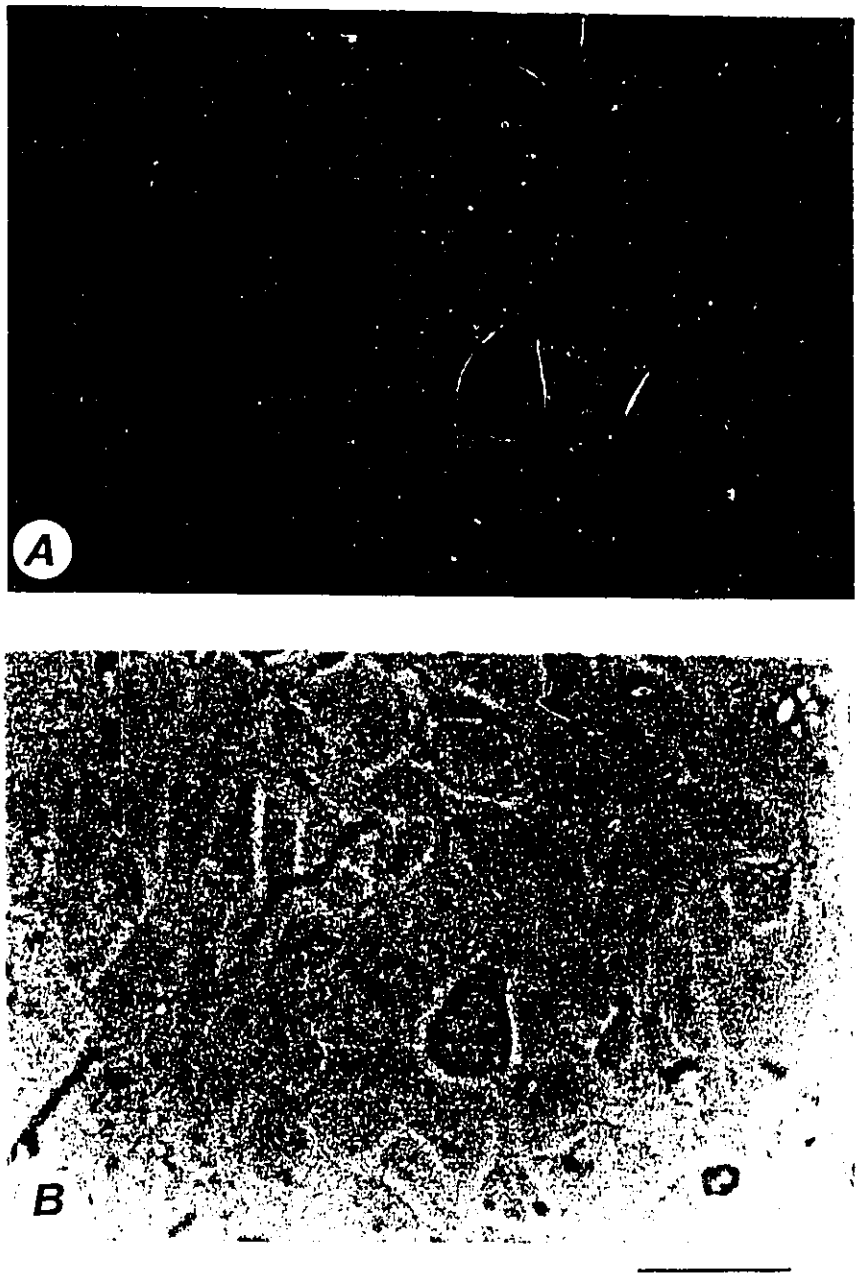

Figure 5.05

Fluorescence micrograph of transfected CCD cells labelled with A: mAb 703 (PC antibody) followed with FITC-labelled anti-mouse immunoglobulin (Ig). B: phase contrast micrograph of (A). 9.6% ± 2 of cells immunoreacted with mAb 703 as determined by image analysis of 10 random fields. Scale bar: 50 μm.

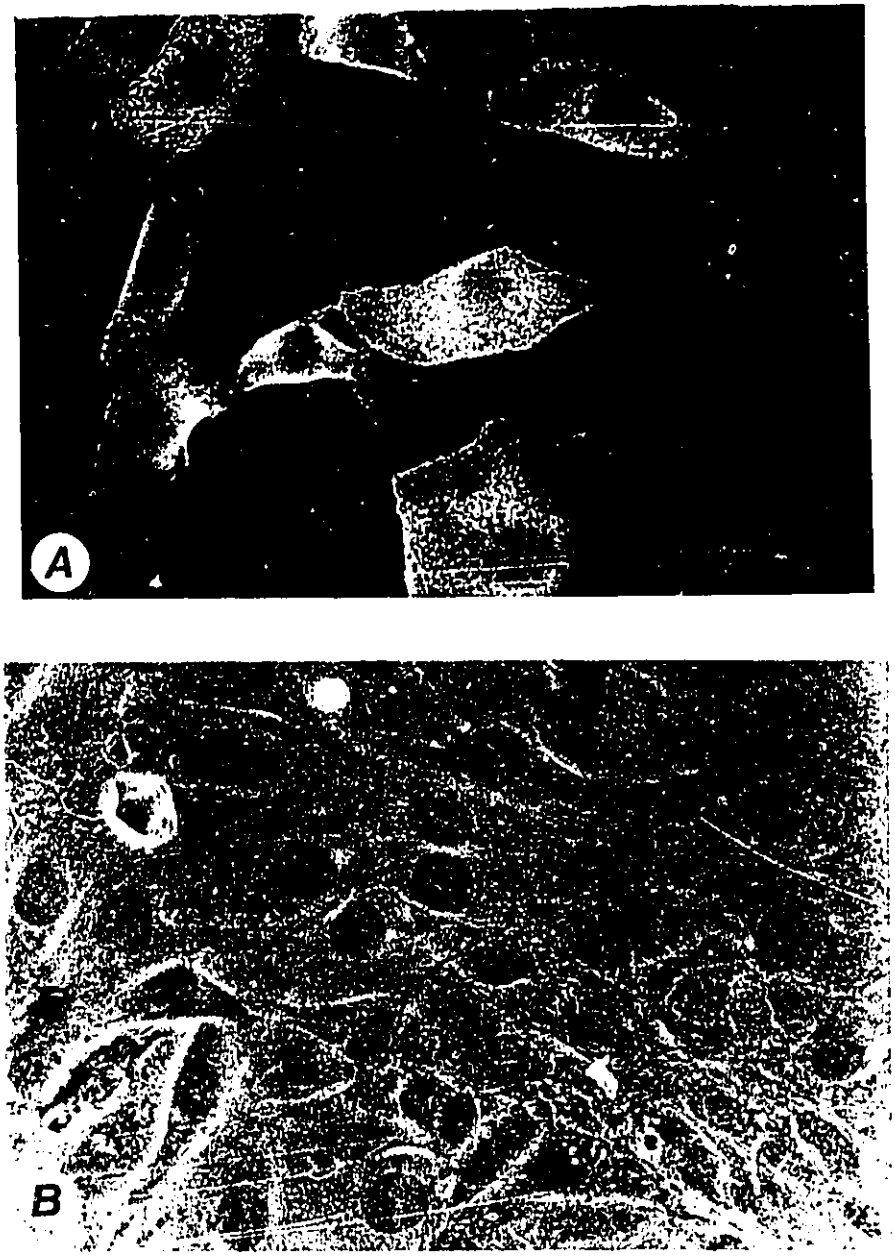

Figure 5.06

Fluorescence micrograph of transfected CCD cells labelled with A: mAb 503 (IC antibody) followed with FITC-labelled anti-mouse Ig. **B:** phase contrast micrograph of (**A**). 16.2 % ± 6 of cells immunoreacted with mAb 503 as determined by image analysis of 10 random fields. Scale bar: 50 μm.

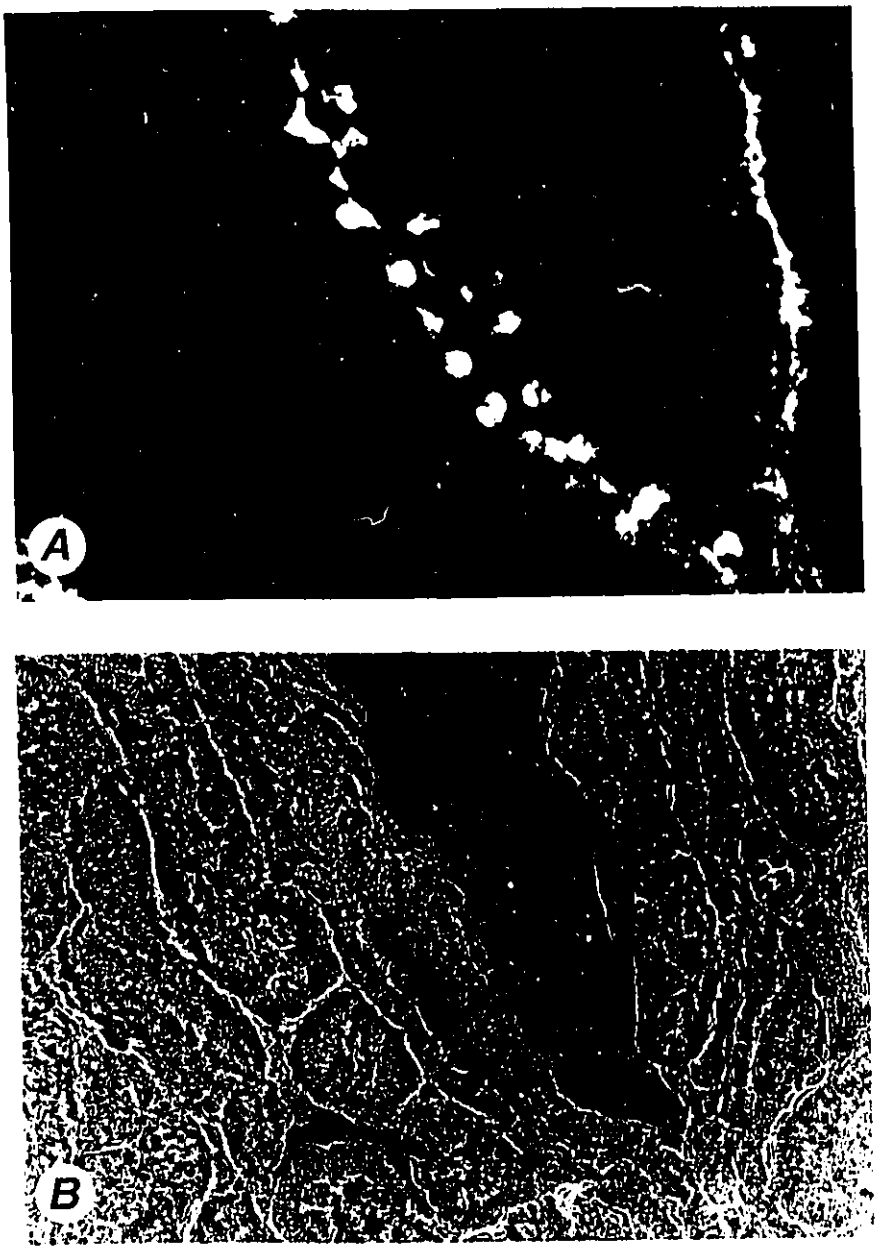

Figure 5.07

Immunofluorescence of mAb 703 in rabbit kidney section. A: Fluorescence micrograph of rabbit kidney section (14 μm) incubated with mAb 703 followed with FITC-labelled anti-mouse Ig. This is a view of the cortical area of the section in which two tubules display intense immunofluorescence. Certain tubules displayed immunofluorescence along their entire length (from cortex to inner medulla) B: Phase contrast of (A). Scale bar: 50 μm.

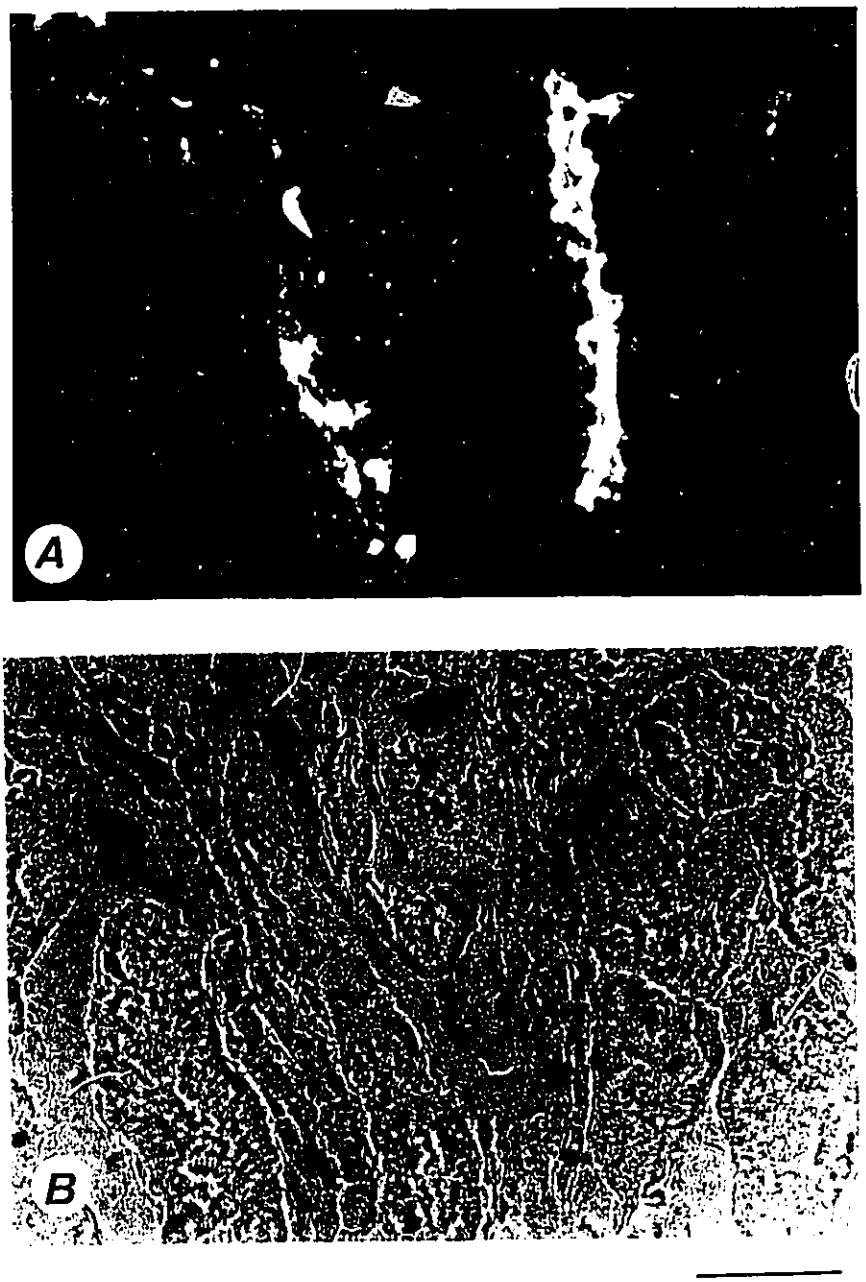

Figure 5.08

Immunofluorescence of mAb 503 in rabbit kidney section. A: Fluorescence micrograph of rabbit kidney section (14 μm) incubated with mAb 503 and secondary FITC labelled anti-mouse Ig. In this field, two tubules immunoreacted with mAb 503 and fluorescence was restricted to the cortical area. The punctuated pattern of fluorescence observed is consistent with mAb 503 labelling of intercalated cells. B: Phase contrast of (A). Scale bar: 50μm.

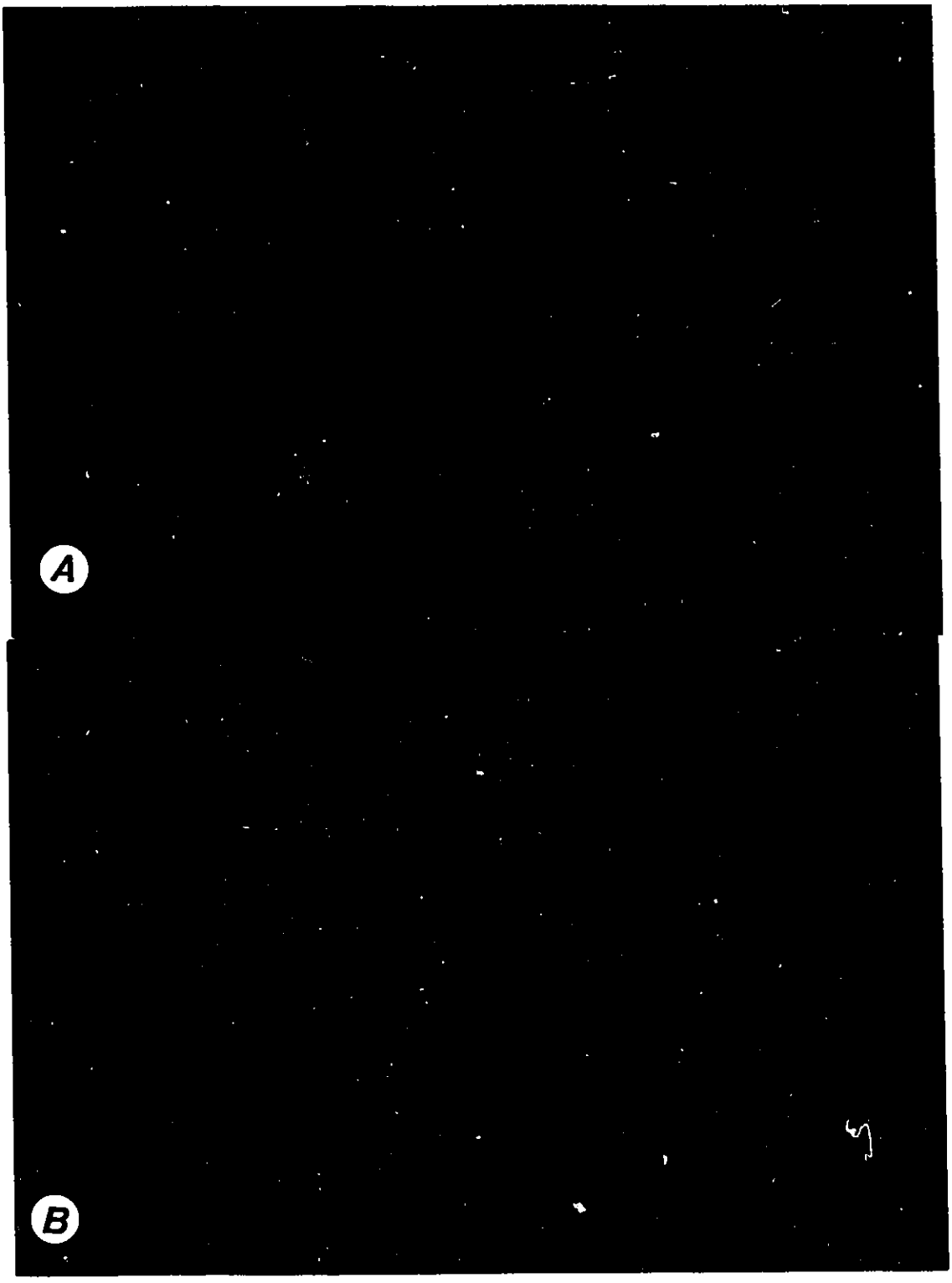

Figure 5.09

Fluorescence micrographs of transfected cells labelled with peanut lectin, mAb 503 and mAb 703. A: Fluorescence of transfected cells grown on coverslips and incubated with FITC-labelled PNA (green) B: Fluorescence of transfected cells incubated with mAb 503 and mAb 703 followed by secondary sheep anti-mouse biotin and streptavidin-texas red.

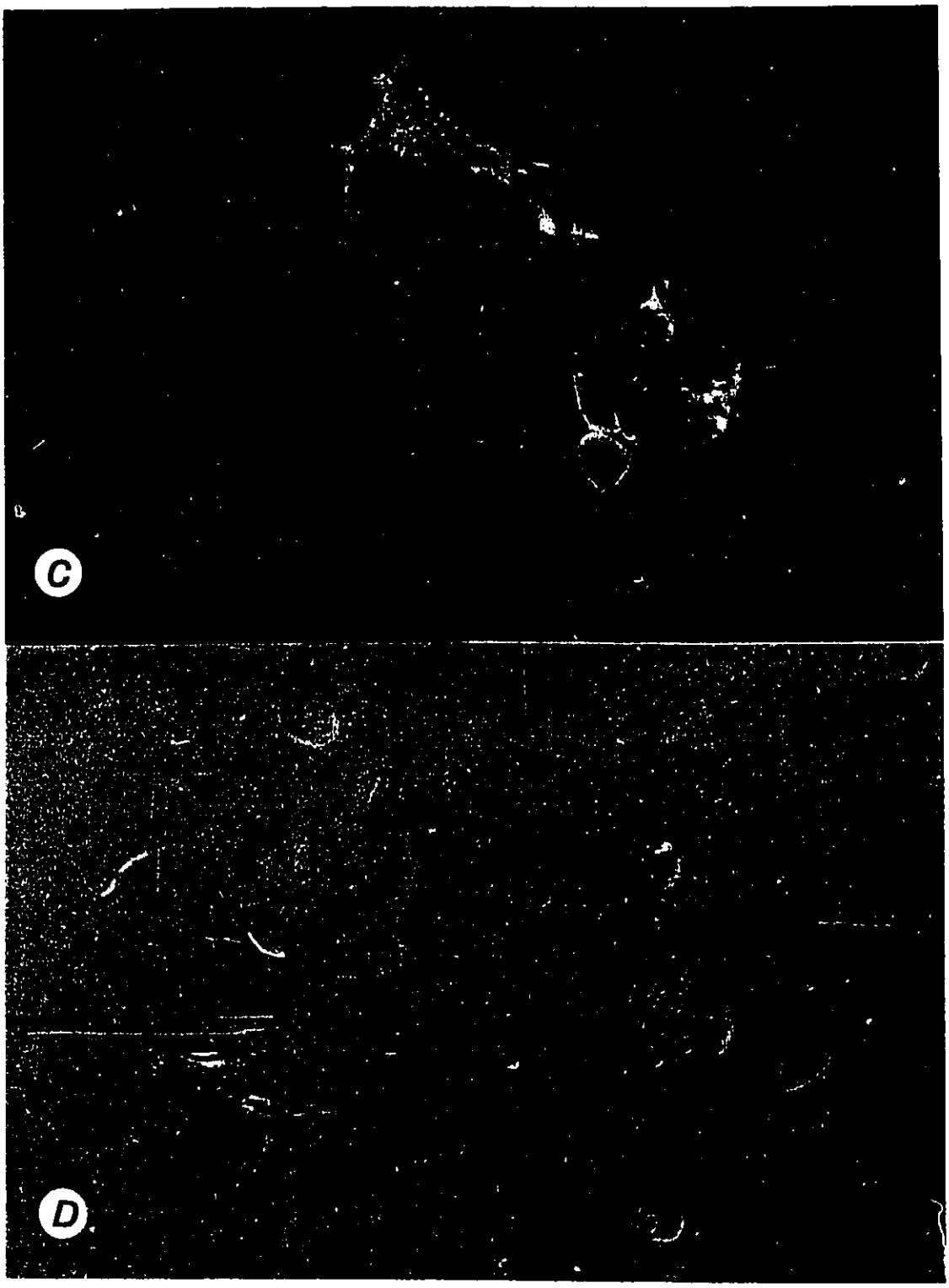

Figure 5.09 (continued)

C: A and B together as seen through a double-label filter. Bright yellow cells immunoreacted with peanut lectin and mAb 503 or mAb 703. D: corresponding Nomarski micrograph of A, B, C. Scale bar: 50 μm.

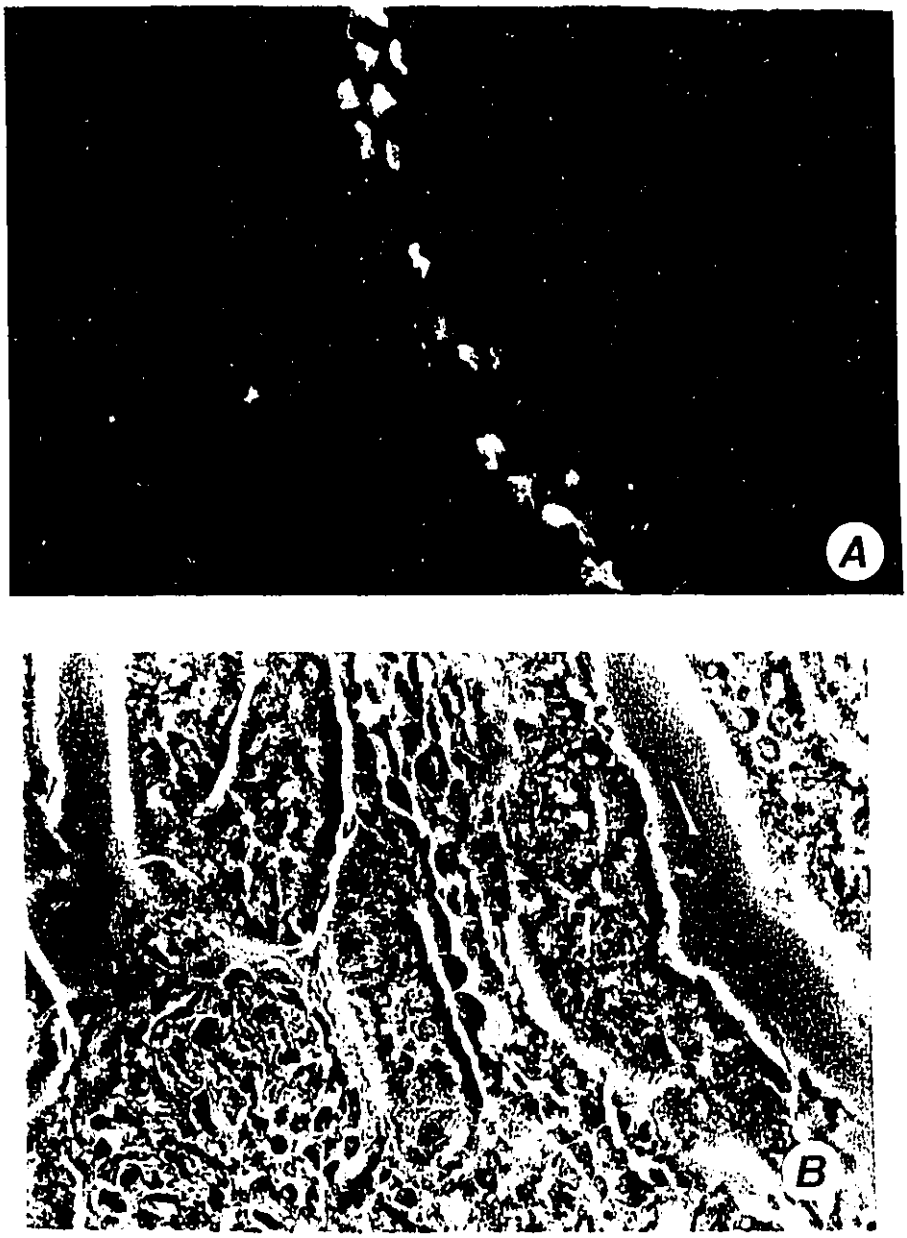

Figure 5.10

Immunofluorescence of Peanut Lectin Agglutinin in rabbit kidney sections.

A: Fluorescence micrograph of rabbit kidney section (14 μm) incubated with FITC-labelled peanut lectin. The pattern of fluorescence observed corresponds to peanut lectin agglutinin labelling of ß-ICs in the CCD. A glomerulus visible in the bottom left hand corner displays no immunoreactivity. B: Phase contrast micrograph of A. Scale bar 50 μm.

Part II

Angiotensin II Studies

5.6 Alkaline Phosphatase Assay

Prior to binding studies, it was important to determine that proximal tubule cells were not contaminating this immortalized cell line, since proximal tubule contains Ang II receptors (Brown et al. 1983, Douglas et al. 1990). A histochemical assay for non-specific alkaline phosphatase, was performed on the transfected cells. Whereas primary cultures of rabbit proximal tubule cells displayed 100% positivity by color reaction (typical of proximal tubule epithelium (Nuyts et al. 1992)), the transfected CCD cell line demonstrated no reactivity (results not shown).

5.7 ^{125}I-Ang II Binding

In transfected CCD cells, radioligand binding assays with Scatchard analysis revealed a single class of Ang II receptors, with an affinity constant (K_d) of 0.78 nM and B_{max} of 90.4 fmol/mg protein (n=2) (Figure 5.11 A). To determine if these receptors were of the AT_1 class, Northern analysis, using a cDNA probe for the rabbit AT_1 Ang II receptor (Burns et al. 1993), was performed on RNA isolated from the immortalized cells. Probe hybridization to membranes containing total RNA derived from these cells was not observed. However, when mRNA was purified by oligo $(dT)^+$ cellulose chromatography, a distinct hybridization signal was observed at 2.3 kb (lanes 1,2) (Figure 5.11 B). This corresponds to the AT_1 Ang II receptor mRNA, as revealed in a positive control of RNA from rabbit kidney cortex (lanes 3,4). In addition, RNase protection assay revealed the presence of AT_1 receptor mRNA in these cells (not shown).

5.8 Effect of Ang II on AVP-Stimulated cAMP Accumulation

Ang II has been reported to inhibit cAMP production in various cells, including rabbit proximal tubules, perhaps via activation of inhibitory G proteins (G_i) (Douglas et al. 1990, Crabos et al. 1994, Harris 1992). To determine if this signalling pathway was present in the immortalized CCD culture, cells were incubated with AVP (10^{-7}M) in the absence and in the presence of Ang II (10^{-7}M) (Figure 5.12). AVP significantly increased cAMP levels (control: 20.4 ± 15.6 vs AVP: 133.2 ± 7.2 pmol/mg protein; $p<0.005$; n=3). When cells were incubated with Ang II at the time of addition of AVP, significant inhibition of AVP-stimulated cAMP production was observed (AVP + Ang II: 105.7 ± 2.1 pmol/mg protein; $p<0.05$; n=3).

5.9 Assay of Phosphoinositide Hydrolysis

In vascular smooth muscle cells, Ang II activates phospholipase C, leading to production of inositol phosphates (Smith et al. 1984). To determine if this pathway was present in the immortalized cell line, cells were incubated with increasing concentrations of Ang II, followed by assay of inositol phosphates. Ang II (10^{-12} - 10^{-9} M) stimulated production of inositol phosphates (Figure 5.13). However, by t-test with Bonferroni correction, this stimulation reached statistical significance only at 10^{-12} M Ang II (123.5 ± 6.6 % above control; $p<0.05$; n=8).

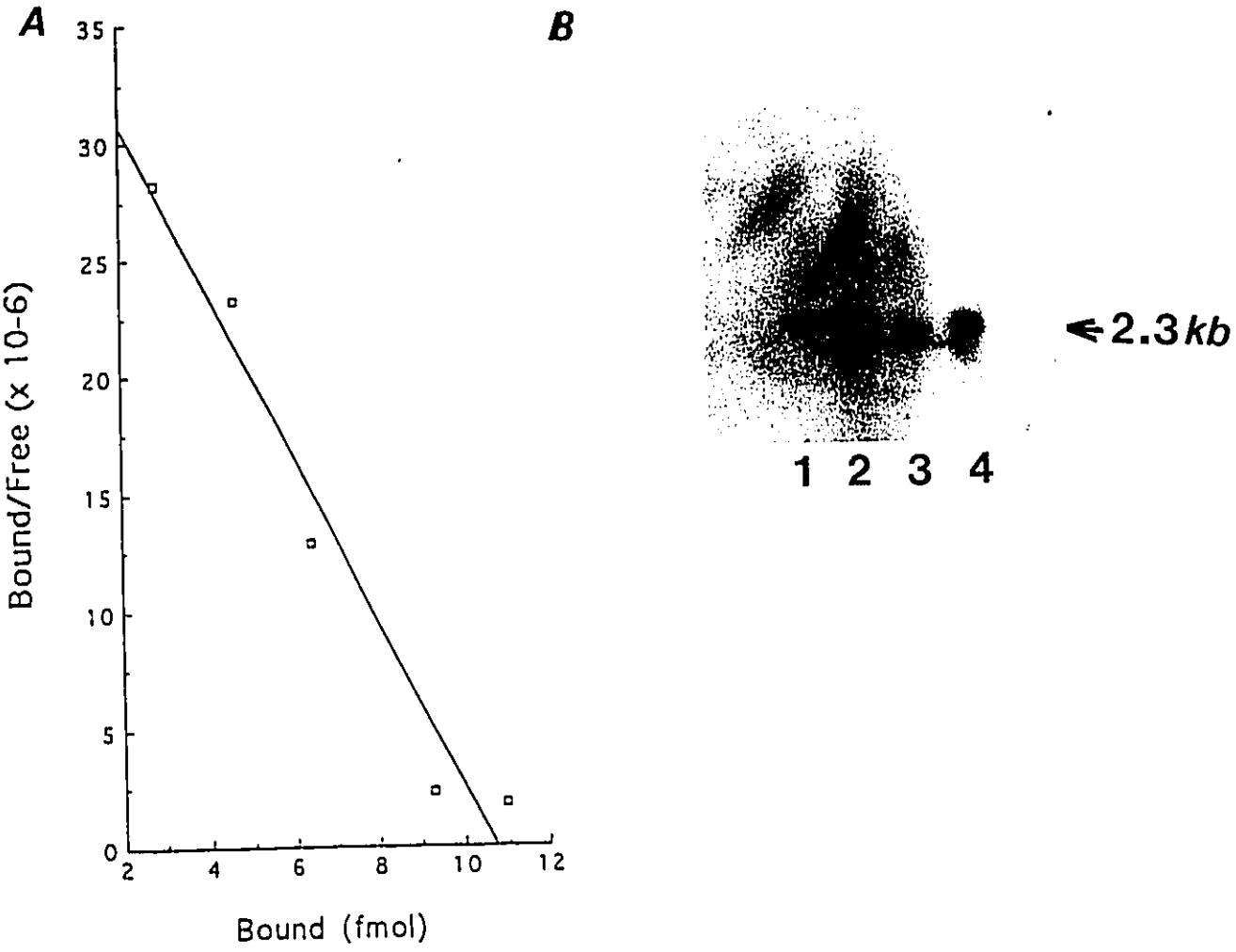

Figure 5.11

Binding of ^{125}I-Ang II to CCD cells. A: Scatchard analysis of ^{125}I-Ang II binding data (K_d= 0.78 nM, B_{max}= 90.4 fmol/mg protein). B: Northern blot analysis for AT_1 receptor mRNA isolated from transfected CCD cells. Lanes 1 and 2 contain 2 μg and 10 μg of transfected CCD cell poly(A)$^+$ RNA respectively, and lanes 3 and 4 contain 5 μg and 20 μg respectively of total RNA isolated from rabbit cortex (positive controls).

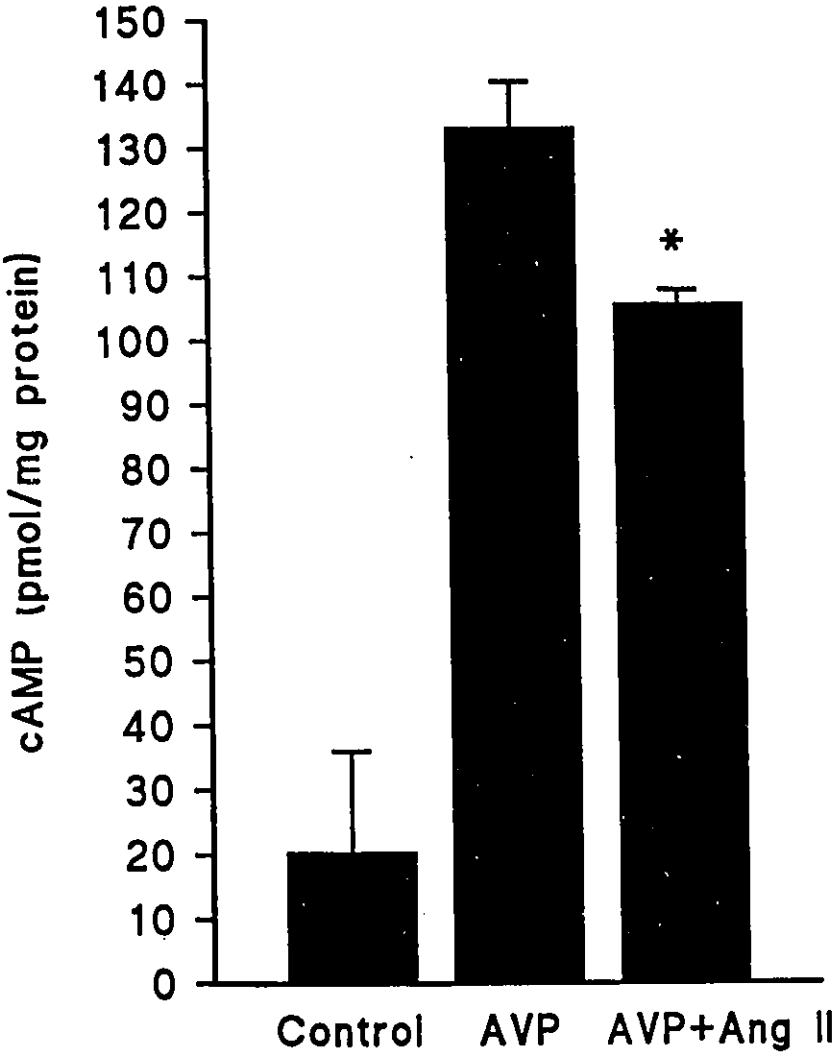

Figure 5.12

Effect of Ang II on AVP-stimulated cAMP accumulation. Cells were incubated with vehicle (CTL), AVP (10^{-7}M) alone or with AVP in the presence of Ang II (10^{-7}M). cAMP levels were determined by radioimmunoassay. n=3, *$p<0.05$ vs AVP alone.

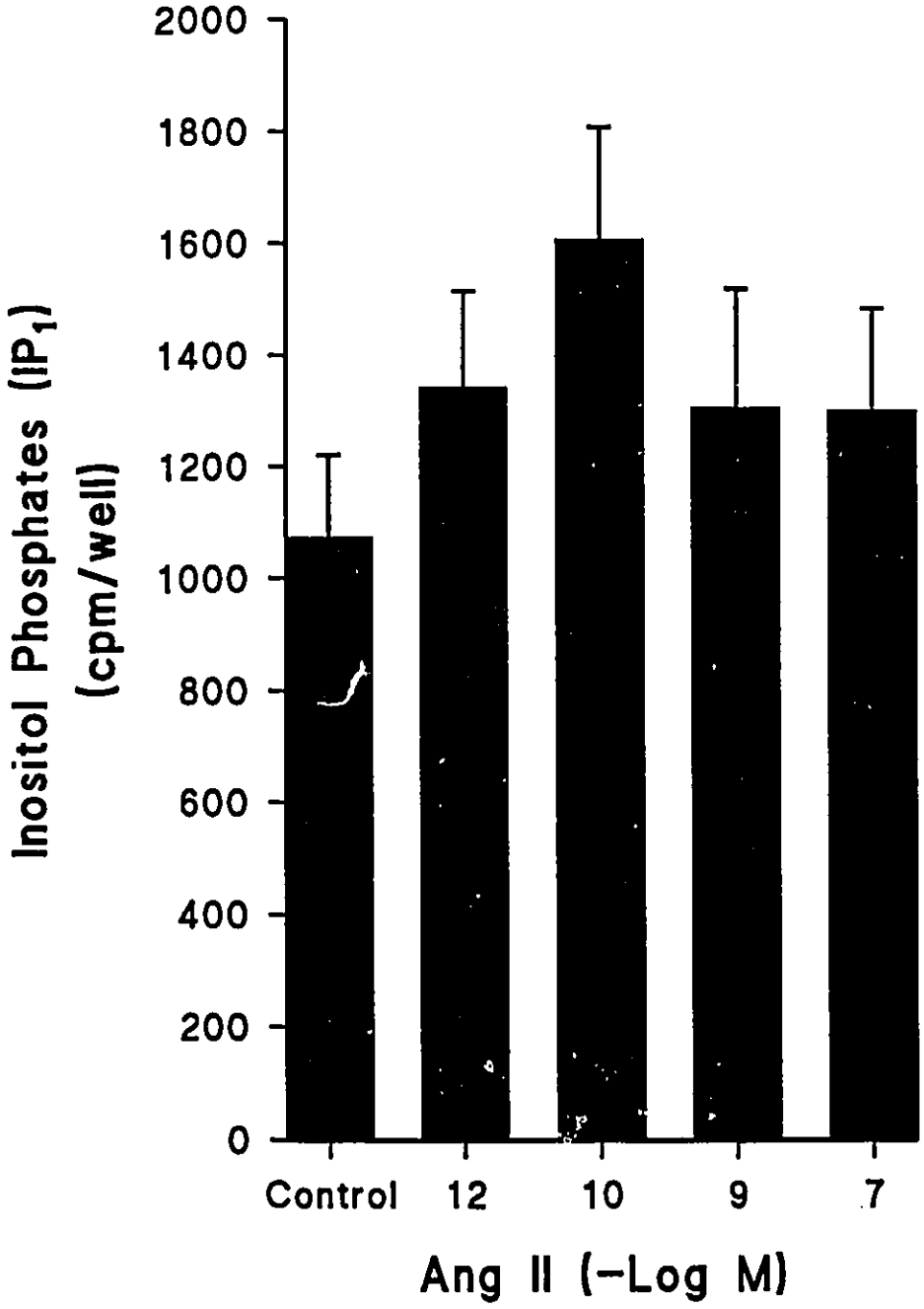

Figure 5.13

Effect of Ang II on phosphoinositide (PI) turnover in transfectd CCD cells. Cells were preincubated with ^{3}H-myo inositol for 72 hours then incubated with various concentrations of Ang II in the presence of LiCl (10mM). Results are means ± SEM, n=4-8.

CHAPTER 6

DISCUSSION

6.0 Summary

In the present study, I have used a novel method to isolate rabbit CCD segments (Lajeunesse et al. 1995) and transfected primary CCD cultures with a plasmid which encodes the large T antigen of SV40 and a G-418 resistance gene. The transfected cells expressed the SV40 large T antigen, displayed peanut lectin agglutinin immunoreactivity, and bound monoclonal antibodies specific for IC (Mab 503) and PC (Mab 703). SEM confirmed the presence of morphologically distinct cell types resembling IC and PC. The hormonal responsiveness of the transfected cells, determined by production of cAMP, was characteristic of CCD segments. This work facilitated studies on Ang II signalling pathways in the CCD. Binding studies revealed the presence of a single class of AT_1 Ang II receptors on these cells. Furthermore, the mechanism of action of Ang II in this segment was characterized by inhibition of cAMP production in response to AVP and increased phosphoinositide hydrolysis.

Therefore, the following discussion will begin by describing the advantages of the procedure used for the isolation of CCD. Second, the conditions used for the culture of CCD and the possible impact on growth and differentiation will be examined. Finally the data with respect to the hormonal, morphological, immunological and Ang II results obtained with the transfected CCD cells will be evaluated.

6.1 CCD Isolation Procedure

Several methods have been developed for the isolation of CCD segments. Microdissection is a technically difficult method which requires special training, the use of

sophisticated equipment and results in low yield (Imbert et al. 1975). Immunodissection is somewhat more advantageous because the yield is greater. However, connecting and collecting tubules share similar surface antigens which react with the same monoclonal antibodies, resulting in contamination (Bindels et al. 1991, Fejes-Tóth et al. 1987). The hormonal profile of cell lines obtained from immunodissected CCD reflects contamination with connecting tubule cells (Arend et al. 1989). Furthermore, the generation of monoclonal antibodies can be time consuming. Therefore, our laboratory developed a simple and effective procedure for the isolation of CCD segments.

Percoll gradients had previously been employed to prepare heterogenous distal tubule populations (Vinay et al. 1981). This undesirable heterogeneity was due to a technical drawback: a wide variation in small densities obtained within a short length of the gradient. The method developed in our laboratory utilized a Ficoll gradient to extend the length over which such densities could be separated. This additional step was effective in separating enriched suspensions of collecting tubules from distal and connecting tubules. The hormonal, functional and immunological evaluation of fresh segments obtained with this method were characteristic of CCD (Lajeunesse et al. 1995). Thus, CCD segments obtained with this method were used for the culture and immortalization of CCD cells.

6.2 Advantages of Cell Cultures and Immortalized Cell Lines

Two major advantages of using tissue culture are the precise control of the physicochemical environment (pH, temperature, osmotic pressure, O_2 and CO_2 tension), and of physiological conditions. Cultures may be exposed directly to a reagent at a lower well

defined concentration without concern for loss by excretion or distribution to tissues other than those under study. Furthermore, the legal, moral and ethical questions of animal experimentation are avoided.

Permanent cell lines offer an additional advantages over primary cultures. First, they eliminate the need for repeated isolation of cells because they may be passaged a number of times without loosing their differentiated characteristics. Second, they reduce "batch" variability associated with primary cultures. Finally, they have accelerated growth rates permitting the rapid expansion of cells for mass experiments.

Nevertheless, the validity of the cultured cell as a model of physiological function *in vivo* has frequently been criticized. Problems of characterization due to the alteration of the cellular environment are routinely encountered; cells proliferate *in vitro* that would not normally *in vivo*, cell-cell and cell-matrix interactions are reduced because purified cell lines lack the heterogeneity and three dimensional architecture found *in vivo*, and the hormonal and nutritional milieu is altered. This may create an environment that favours the spreading, migration, and proliferation of unspecialized cells rather than the expression of differentiated functions. However, the provision of the appropriate environment, nutrients, hormones, and substrate can counter these difficulties by stimulating the expression of specialized functions. These factors were taken into careful consideration in the selection of culture conditions for CCD primary cultures and immortalized cells as described in methods. The culture media selected (DMEM/HamF12) contains a large number of different amino acids, including non-essential amino acids, vitamins, minerals and glucose. Furthermore, the media was supplemented with a number of hormones and serum: 1) fetal

bovine serum which has been demonstrated to increase epithelial permeability in epithelial cell lines (Mortell et al. 1993) 2) insulin which has a mitogenic effect on cultured cells and improves plating efficiency (Hamilton et al. 1977) 3) hydrocortisone which is used to promote cell attachment (Fredin et al. 1979) proliferation (McLean et al. 1986), and differentiation (Speirs et al. 1991). In addition, Barnes and Sato (1980) described the use of 5-tri-iodo thyronine (T_3) as a necessary supplement for MDCK cells. The above conditions promoted the conservation of hormonal, morphological and antigenic properties of transfected CCD cells, as will be discussed in the following sections.

6.3 Hormonal Responses

Hormone-induced cAMP production in the immortalized cells was characteristic of intact CCD, and similar to responses recently reported in freshly isolated CCD segments using this separation method (Lajeunesse et al. 1995). In transfected CCD cells, increases in cAMP in response to AVP and PGE_2 were observed, likely mediated by V_2 and EP_2 receptors respectively (Breyer et al. 1990), which may reside on PC (Kirk 1988, Brown et al. 1983). The magnitude of the production of cAMP in response to AVP was 10-fold greater than that to PGE_2. In this regard, it is of interest that AVP is significantly more potent than PGE_2 in stimulating water permeability in microperfused CCD (Grantham et al. 1968). The precise membrane distribution of these receptors, basolateral versus apical, on the transfected CCD cells is at the present time unknown.

Our cell line differs from the RCCT 28A rabbit CCD cell line (Arend et al. 1989) in that it does not respond to sCT or PTH. These hormones elicit production of cAMP in

distal and connecting tubule segments (Charbadès et al. 1975, 1976). Therefore, the lack of such a response in our cell line suggests an enhanced enrichment with CCD cells.

6.4 AVP and PGE_2 Dose Response Curves

The EC_{50} (6.2 nM) for AVP-stimulated cAMP production in the transfected cells was 10-fold lower than previously reported in microdissected CCT (Imbert et al. 1975, Torikai et al. 1983, Charbardès et al. 1988). This discrepancy was not unexpected given that culturing of cells has been reported to cause the downregulation of AVP receptors (Bouscarel et al. 1990). Sonnenburg et al. (1988) reported that high concentrations of PGE_2 increased cAMP production in cultured rabbit CCD cells (EC_{50} approximately 0.1 μM). These results are similar to those observed with our transfected CCD cells (EC_{50} 0.17 μM).

The reader should be reminded that the following discussion on the results obtained with PGE_2 analogues and PGE_2 mediated "inhibition" of AVP-stimulated cAMP production are preliminary. The EP_2 receptor selective analogue, Butaprost was also capable of increasing cAMP production in transfected cells. This suggests that the immortalization of CCD cells did not in any way interfere with the expression and function of the EP_2 receptor subtype.

In contrast, sulprostone, an EP_3 receptor selective analogue of PGE_2, did not increase cAMP production in the transfected CCD cells. This result was not unexpected given that sulprostone has no effect on basal hydraulic conductivity in the CCD (Hébert et. al. 1993). However, preliminary data suggests that the EP_3 receptor subtype is absent or dysfunctional. The EP_3 receptor subtype is coupled to an inhibitory G protein (Gi) which is linked to the

adenylate cyclase. When PGE_2 and AVP were applied in combination, a significant increase in cAMP levels from AVP alone was observed (Table 5.2). The predicted response would have been inhibition of AVP-stimulated cAMP by PGE_2 if functional EP_3 receptors were present. It is possible that the dose of AVP (10^{-8}M), and the length of time of preincubation were not optimal for these purposes. These possibilities are now being explored. Nevertheless, similar results were obtained by Sonnenburg and colleagues (1988) in which PGE_2 and sulprostone failed to inhibit AVP-stimulated cAMP accumulation in a primary culture of CCD cells. Two possible explanations for this paradox are: 1) the EP_3 receptor is not expressed by the transfected CCD cells or 2) the lack of inhibition of AVP-stimulated cAMP production by PGE_2 and SLP is due to an uncoupling of the inhibitory G protein (Gi) to its receptor.

The presence of EP_1 receptor subtypes was not examined in this study. These receptor subtypes are coupled to the phospholipase C signalling cascade. Thus, it remains to be determined whether EP_1 receptor subtypes are present and functional with respect to having retained the ability to activate phospholipase C in these cells.

6.5 Morphological Characterization

Despite the fact that the hormonal responses characteristic of intact CCD were retained by the transfected CCD cells; phase contrast microscopy and SEM were performed to determine whether the morphology of the cells was retained as well.

The general appearance of the transfected cells in culture was observed with low magnification phase contrast microscopy. Cells formed a single layer (monolayer) on the

surface of the glass coverslip and displayed "epithelioid" morphology (Freshney 1994). Furthermore, dome formations were observed on several occasions. Dome formation occurs when the cell layer on an impermeable substratum is pushed away from the culture dish by the accumulation of fluid beneath (Rabito et al. 1980). This suggests that the monolayer is a polarized epithelium displaying vectorial transport of ions and water.

The results of SEM revealed cells with distinct cell surface patterns resembling those of PC and IC. Cells either had a microplicated surface, as described for α-IC (Verlander et al. 1987, Evan et al. 1991), or a surface with short microvilli, as seen in PC or ß-IC (Evan et al. 1991, Lefurgey et al. 1979). The presence of a single cell cilium has been described in both PC from microdissected CCD (Evan et al. 1991, Lefurgey et al. 1979) and in primary cultures of CCD cells (Jamous et al. 1993, Herter et al. 1993). In our transfected cells, cilia were absent on SEM. However, this was not an unexpected finding. Cilia were not described in morphological studies of a permanent PC cell line (RC.SVtsA58) (Prié et al. 1994) or in a mouse CCD cell line (Stoos et al. 1991), indicating that the loss of this phenotype may be a consequence of immortalization or repeated passages. In fact, the expression of the SV40 genome in mammalian cells has previously been reported to cause phenotypic alterations in other SV40-transformed cell lines (Cherington et al. 1986, Garcia et al. 1986, Amsterdam et al. 1988).

Alternatively, the absence of cilia may represent inadequate supplementation of the culture media with growth factors and/or hormones to stimulate the differentiated growth of cilia on principal cells. This seems unlikely given that culture conditions were selected to optimize the differentiation of CCD cells, the maintenance of morphological features and

the preservation of specialized functions. Nevertheless, Minuth reported that aldosterone influences the differentiation of principal cells in culture. The culture media was not supplemented with aldosterone which may or may not be present in fetal bovine serum. Rather, the culture was supplemented with hydrocortisone a known promoter of cell differentiation in culture (Speirs et al. 1991).

6.6 Immunological Characterization

6.6.1 Large T Antigen

In order to assess whether all cells had been successfully transfected with the SV40 plasmid which encodes the large T antigen, we determined if the large T antigen was expressed in these cells by immunocytochemistry. The observation that 100% of the cell nuclei immunofluoresced when incubated with large T antigen antibodies, demonstrated that all cells incorporated the plasmid. This was performed twice on cells of passage 3 and passage 8 and both times 100% nuclear immunoreactivity was observed suggesting that passaging does not interfere with the propagation of the plasmid DNA.

6.6.2 mAb 503, mAb 703 and Peanut Lectin Agglutinin

We utilized immunofluorescence labelling with mAb 703 and mAb 503 to determine if transfected CCD cells expressed PC and IC surface antigens, respectively. Notably, the overall percentage of positively-stained cells (~25%) was less than that observed in rabbit kidney sections (Tauc et al. 1992). However, using these antibodies, Tauc et al. reported

a progressive decline of greater than 20% in expression of these markers in CCD cells in primary culture (Tauc et al. 1992). Thus, we did not anticipate that our immortalized cells would retain 100% positivity.

Of the three markers utilized in the present study, peanut lectin agglutinin, a ß-IC marker, identified the greatest proportion of cells (~27%). We also observed cells which double-labelled with both peanut lectin and with either mAb 703 or mAb 503. In this regard, it is noteworthy that other investigators (Jamous et al. 1993, Fejes-Tóth et al. 1992) have postulated that CCD cells might interconvert, suggesting that cross-expression of surface antigens might occur during this process. Furthermore, the existence of a third type of IC (γ-IC) has recently been reported in functional studies in rabbit outer CCD (Emmons et al. 1994). These cells appear to express both apical and basolateral Cl^-/HCO_3^- exchange, suggesting an intermediate function between α-IC and ß-IC (Emmons et al. 1994). Alternatively, it is possible that our results may reflect nonspecificity of antibodies or dedifferentiation of transfected cells.

When transfected CCD cells were incubated with all three of mAb 503, mAb 703, and peanut lectin, approximately 50% of cells remained unlabelled. We postulate that the majority of nonreactive cells represent dedifferentiated CCD cells, for three reasons: 1) all cells retained morphological surface characteristics of CCD cells 2) alkaline phosphatase staining was negative, suggesting absence of contamination with proximal tubular cells, and 3) hormonal responses were characteristic of CCD, and exclude significant presence of distal tubule or connecting segment cells. Nevertheless, the present studies do not exclude the possibility that some nonreactive cells represent contaminating cells of tubular or non-tubular origin.

6.7 Role of Angiotensin II in the CCD

In the present study, we initially characterized the role of Ang II in the CCD. Binding experiments detected the presence of a single class of Ang II receptors in transfected rabbit CCD cells. The affinity constant (K_d 0.78nM) and B_{max} (90.4 fmoles/mg protein) were characteristic of high affinity AT_1 receptors (Brown et al. 1983, Burns et al. 1993). In addition, Northern analysis demonstrated the mRNA for the AT_1 receptor subtype. Since the purpose of this study was to determine the presence of well-defined signalling pathways for Ang II in these cells, our studies did not assay for presence of AT_2 Ang II receptors. Therefore, we cannot exclude their presence in immortalized CCD cells.

In order to identify the signal transduction mechanisms of Ang II in the transfected CCD cells, cAMP production and phosphoinositide turnover in response to Ang II stimulation was measured. Ang II caused significant inhibition (20.2 %) of AVP-induced cAMP formation in transfected CCD cells. This is indicative of Ang II-mediated adenylate cyclase inhibition via an AT_1 receptor coupled to an inhibitory G protein (Gi) as was previously demonstrated to occur in the proximal tubule (Douglas et al. 1990). Cultures of proximal tubule cells appear to be more sensitive with regard to the fact that 1 nM Ang II was required to achieve a 34% inhibition of cAMP production (Douglas et al. 1990). In other cell types, including proximal tubule epithelium, AT_1 receptors are coupled to phospholipase C which catalyses the breakdown of PIP_2 to phosphoinositides (IP_1, IP_2, IP_3) and DAG (Burns et al. 1995, Crabos et al. 1994) when activated by Ang II. Ang II caused increases in phosphoinositide turnover in the transfected CCD cells providing additional evidence of an AT_1 mediated response. Interestingly, the stimulation did not reach

statistical significance, which may be due to high daily variability resulting in a large SEM. The basis for the apparent lack of concentration-response may relate to complex signalling pathways for Ang II in CCD, as have been described in proximal tubule (Douglas et al. 1990). In this regard, the role of possible increases in intracellular calcium with high concentrations of Ang II requires further study. Overall, the results are consistent with Ang II acting through an AT_1 receptor subtype as opposed to the AT_2 receptor subtype because the latter has not been shown to be linked to these pathways.

6.8 Previously Established CCD Cell Lines: A Comparison

A number of CCD cell lines have been developed. The first rabbit CCD cell line established by Arend et al. (RCCT28A) was derived from immunodissected CCD cells. In contrast to our CCD cell line, the RCCT28A cell line did not retain the hormonal characteristics of CCD. Stoos and coworkers (1991) have used a mouse transgenic for the early region of SV40 to create an immortalized mouse CCD cell line (M-1). The Madin-Darby canine kidney cell line (MDCK) has also been described as a CCD cell line (Devuyst et al. 1994). However, in contrast to the rabbit which has been used extensively to study CCD physiology, the mouse and dog have rarely been used and would therefore not provide a useful models for reference purposes. Interestingly, Prié and coworkers (1994) claim to have developed a rabbit principal cell line (RC.SVtsA58) from primary cultures of tubular cortical cells expressing essentially proximal cell functions. In addition, Edwards and coworkers (1992) immortalized rabbit bicarbonate-secreting cells with a temperature sensitive strain of SV40 (IC250). The latter would only be useful for the study of ß-

intercalated cells. Given the inadequacies of previously established CCD cell lines, the rationale for having developed a more reliable rabbit CCD cell line is self evident. In brief, our rabbit CCD cell line has been extensively characterized and is the only rabbit CCD cell line reported to express functional AT_1 Ang II receptors.

6.9 Future Directions

Ang II has recently been shown to stimulate H^+-ATPase activity in rat CCD (Tojo et al. 1994), and to increase net HCO_3^- reabsorption in rat distal tubule, *in vivo* (Levine et al. 1994). Thus, these data suggest that AT_1 Ang II receptors may be present on α-IC, which mediate HCO_3^- reabsorption via the apical H^+APTase. However, further studies are required to precisely locate these receptors in rabbit CCD cells, and to determine if they are distributed on luminal and basolateral surfaces, as in proximal tubule (Douglas et al. 1990). It would also be of interest to examine the influence of Ang II on HCO_3^- transport in transfected CCD cells which can be grown on semi-permeable supports. Other experiments may involve the use of the AT_1 receptor antagonist Losartan (DuP 753) to determine if inhibition of adenylate cyclase and phosphoinositide turnover can be completely or partially abolished. The possibility that these cells express the AT_2 Ang II receptor subtypes should also be addressed. Although the expression of AT_2 receptor subtypes is unlikely given that this receptor is only expressed in the fetal kidney, it is possible that in culture, CCD cells revert to a more primitive form.

6.10 Conclusions

Interest on the effects of Ang II on the collecting duct in both physiological and pathophysiological states is steadily growing. The demonstration of Ang II mediated cell hypertrophy during K^+ depletion was instrumental in bringing this subject to the research forefront (Mujais 1994). It was one of the first studies to document that ACE inhibition had a direct tubular renoprotective effect as opposed to a haemodynamic renoprotective effect. Considering the importance of tubular hypertrophy in the progression of renal failure in many models, strategies to block the action of Ang II on tubular cells may offer an attractive alternative way to control deterioration of renal function besides modulation of haemodynamics. The development of therapeutic strategies to block the action of Ang II on tubular cells will require precise knowledge of Ang II mechanisms of action on various nephron segments. In this regard, the present study will provide valuable information of Ang II signal transduction mechanisms in the CCD.

Although this study focused on Ang II interactions in CCD, the potential uses for this cell line are vast. Recently a number of CCD water channels have been cloned, WCH-CD or Aquaporin-2 (Fushimi et al. 1993), Aquaporin-3 (Ma et al. 1994) and BLIP (Valenti et al. 1994). This cell line may be instrumental for studying the expression and function of these water channels in principal cells. Also, given the apparent heterogeneity of this cell line, it may be possible to examine the plasticity of α and ß intercalated cells and to test the interconversion hypothesis. Furthermore, pure α-IC, ß-IC, and PC cell lines may be prepared by subcloning of our heterogenous CCD cell line. Finally, this cell line will render the study of the biochemical and functional effects of numerous hormones, growth factors on the CCD relatively effortless.

In conclusion, this is the first characterization of a rabbit cortical collecting duct cell line which retains the hormonal responsiveness and expresses specific antigens and morphological characteristics of both PC and IC. This CCD cell line expresses functional AT_1 Ang II receptors linked to well-known signal transduction pathways and may provide further insight into the physiological role of Ang II in the CCD.

This work was granted the Canadian Society of Nephrology Trainee Award and was presented in part at the annual meetings of the Canadian Society of Clinical Investigation (CSCI) and of the American Society of Nephrology (ASN) in 1994 (Burns et al. 1994). Since, I have received several demands for this cell line. Ongoing research in Dr. Skorecki's lab is examining the expression of the aquaporin-2 gene in these cells and Dr. Stephen Gluck is carrying out immunohistochemical studies to determine the expression of H^+ATPases in these cells.

CHAPTER 7

REFERENCES

Alexander RW, Brock TA, Gimbrone JR MA, Rittenhouse SE: Angiotensin increases inositol trisposphate and calcium in vascular smooth muscle. *Hypertension* 7:447-451, 1985.

Alper SL, Natale J, Gluck S, Lodish HF, Brown D: Subtypes of intercalated cells in rat kidney collecting duct defined by antibodies against erythroid band 3 and renal vacuolar H^+-ATPase. *Proc Natl Acad Sci USA* 86:5429-5433, 1989.

Amsterdam A, Zauberman A, Meir G, Pinhasi-Kimhi O, Suh BS, Oren M: Cotransfection of granulosa cells with simian virus 40 and Ha-RAS oncogene generates stable lines capable of induced steroidogenesis. *Proc Natl Acad Sci USA* 85:7582-7586, 1988.

Arend LJ, Handler JS, Rhim JS, Gusovsky F, Spielman WS: Adenosine-sensitive phosphoinositide turnover in a newly established renal cell line. *Am J Physiol* 256:F1067-F1074, 1989.

Ausiello DA, Skorecki KL, Verkman AS, Bonventre JV: Vasopressin signaling in kidney cells. *Kidney Int* 31:521-529, 1987.

Aviv H, Leder P: Purification of biologically active globin messenger RNA by chromatography on oligothymidylic acid-cellulose. *Proc Natl Acad Sci* 69:1408-1412, 1972.

Barnes D, Sato G: Mehtods for growth of cultured cells in serum-free medium. *Anal Biochem* 102:255-270, 1980.

Bastani B, Yang L, Steinhardt G: Immunocytochemical localization of vacuolar H^+-ATPase in the opossum (*Monodelphis domestica*) kidney: Comparison with the rat. *J Am Soc Nephrol* 4:1558-1563, 1994.

Berridge MJ: Inositol trisphosphate and calcium signalling. *Nature* 361:315-325, 1993.

Bindels RJM, Hartog A, Timmermans J, Van Os CH: Active Ca^{2+} transport in primary cultures of rabbit kidney CCD: Stimulation by 1,25-dihydroxyvitamin D_3 and PTH. *Am J Physiol* 261:F799-F807, 1991.

Bloch RD, Zikos D, Fisher KA, Schleicher L, Oyama M, Cheng JC, Skopicki HA, Sukowski EJ, Cragoe EJ Jr, Peterson DR: Activation of proximal tubular $Na(^+)$-H^+ exchange by angiotensin II. *Am J Physiol* 263:F135-F143, 1992.

Bottari SP, King IN, Reichlin S, Dahlstroem I, Lydon N, de Gasparo M: The angiotensin AT_2 receptor stimulates protein tyrosine phosphatase activity and mediates inhibition of particulate guanylate cyclase. *Biochem Biophys Res Comm* 183:206-211, 1992.

Bouscarel B, Augert G, Taylor SJ, Exton JH: Alterations in vasopressin and angiotensin II receptors and responses during culture of rat liver cells. *Elsevier Science Publishers B.V. (Biomedical Division)*, Paris, p 265-272, 1990.

Braun-Menendez E, Fasciolo JC, Leloir LF, Munoz JM: The substance causing renal hypertension. *J Physiol* 98:283-298, 1940.

Breyer MD, Jacobson HR, Hebert RL: Cellular mechanisms of prostaglandin E2 and vasopressin interactions in the collecting duct. *Kidney Int* 38:618-624, 1990.

Breyer MD: Feedback inhibition of cyclic adenosine monophosphate stimulated Na^+ transport in the rabbit cortical collecting duct via Na^+ dependent basolateral Ca^{2+} entry. *J Clin Invest* 88:1502-1510, 1991.

a) **Breyer MD, Ando Y:** Hormonal signaling and regulation of salt and water transport in the collecting duct. *Annu Rev Physiol* 56:711-739, 1994.

b) **Breyer RM, Jacobson HR, Jian C, Abromson R, Breyer MD:** Molecular cloning of a butaprost insensitive prostaglandin receptor (EP4) from rabbit kidney. Abstract *J Am Soc Nephrol* 5:677, 1994.

Brown D, Orci L: Vasopressin stimulates formation of coated pits in rat kidney collecting ducts. *Nature* 302:253-255, 1983.

Brown GP, Douglas JG: Angiotensin II binding sites on isolated rat renal brush border membranes. *Endocrinology* 111:1830-1836, 1982.

Brown GP, Douglas JG: Angiotensin II binding sites in rat and primate isolated renal tubular basolateral membranes. *Endocrinology* 112:2007-2014, 1983.

Burns KD, Harris RC: Signaling and growth responses of LLC-PK_1/Cl_4 cells transfected with the rabbit AT_1 angiotensin II receptor. *Am J Physiol* 268:C925-C935, 1995.

Burns KD, Regnier L, Rockzniak A, Lajeunesse D, Hébert RL: An immortalized rabbit cortical collecting duct (CCD) cell line with functional angiotensin II (Ang II) receptors (Abstract). *J Am Soc Nephrol* 5:656, 1994.

Burns KD, Inagami T, Harris RC: Cloning of a rabbit kidney cortex AT_1 angiotensin II receptor that is present in proximal tubule epithelium. *Am J Physiol* 264:F645-F654, 1993.

Capasso G, Unwin R, Ciani F, De Santo NG, De Tommaso G, Russo F, Giebisch G: Bicarbonate transport along the loop of Henle II. Effects of acid-base, dietary, and neurohumoral determinants. *J Clin Invest* 94:830-838, 1994.

Charbadès D, Imbert-Teboul M, Montégut M, Clique A, Morel F: Distribution of calcitonin-sensitive adenylate cyclase activity along the rabbit kidney tubule. *Proc Natl Acad Sci USA* 76:3608-3612, 1976.

Charbadès D, Imbert M, Clique A, Montégut M, Morel F: PTH sensitive adenylate cyclase activity in different segments of the rabbit nephron. *Pflugers Arch* 354:229-239, 1975.

Charbadès D, Brick-Ghannam C, Montégut M, Siaume-Perez S: Effect of PGE_2 and α-adrenergic agonists on AVP-dependent cAMP levels in rabbit and rat CCT. *Am J Physiol* 255:F43-F48, 1988.

Chen C, Okayama: High efficiency transformation of mammalian cells by plasmid DNA. *Mol Cell Biol* 8:2745-2752, 1987.

Cherington V, Morgan B, Speigelman M, Roberts TM: Recombinant retroviruses that transduce individual polyoma tumor antigens: effects on growth and differentiation. *Proc Natl Acad Sci USA* 83:4307-4311, 1986.

Chomczynski P, Sacchi N: Single-step method of RNA isolation by acid guanidinium thiocyanate-phenol-chloroform extraction. *Anal Biochem* 162:156-159, 1987.

Church GM, Gilbert W: Genomic sequencing. *Proc Natl Acad Sci* 81:1991-1995, 1984.

Crabos M, Roth M, Hahn AWA, Erne P: Characterization of angiotensin II receptors in cultured adult rat cardiac fibroblasts. *J Clin Invest* 93:2372-2378, 1994.

Dean NM, Beaven MA: Methods for the analysis of inositol phosphates. *Analytical Biochemistry* 183:199-209, 1989.

Devuyst O, Beauwens R, Denef JF, Crabbé, Abramow M: Subtypes of Madin-Darby canine kidney (MDCK) cells defined by immunocytochemistry: Further evidence for properties of renal collecting duct cells. *Cell Tissue Res* 277:231-237, 1994.

Dominguez JH, Snowdowne K, Freudenrich CC, Brown T, Borle AB: Intracellular messenger for action of angiotensin II on fluid transport in rabbit proximal tubule. *Am J Physiol* 252:F423-F428, 1987.

Douglas JG, Romero M, Hopfer U: Signaling mechanisms coupled to the angiotensin receptor of proximal tubular epithelium. *Kidney Int* 38:S43-S47, 1990.

Edmonds M, Vaughan MH, Nakazato H: Polyadenylic acid sequences in the heterogenous nuclear RNA and rapidly-labelled polyribosomal RNA of HeLa cells: Possible evidence for a precursor relationship. *Proc Natl Acad Sci* 68:1336-1340, 1971.

Edwards JC, van Aldelsberg J, Rater M, Herzlinger D, Lebowitz J, al-Awqati Q: Conditional immortalization of bicarbonate-secreting intercalated cells from rabbit. *Am J Physiol* 263:C521-C529, 1992.

Elger ML, Bankir L, Kriz W: Morphometric analysis of kidney hypertrophy in rats after chronic potassium depletion. *Am J Physiol* 262:F656-F667, 1992.

Emmons C, Kurtz I: Functional characterization of three intercalated cell subtypes in the rabbit outer cortical collecting duct. *J Clin Invest* 93:417-423, 1994.

Evan AP, Satlin LM, GattoneII VH, Connors B, Schwartz GJ: Postnatal maturation of rabbit renal collecting duct II. Morphological observations. *Am J Physiol* 261:F91-F107, 1991.

Fejes-Tóth G, Naray-Fejes-Tóth A: Differentiated transport functions in primary cultures of rabbit collecting ducts. *Am J Physiol* 253:F1302-F1307, 1987.

Fejes-Tóth G, Náray-Fejes-Tóth A: Isolated principal and intercalated cells: hormone responsiveness and Na^+-K^+-ATPase activity. *Am J Physiol* 256:F742-F750, 1989.

Fejes-Tóth G, Náray Fejes-Tóth A: Differentiation of renal ß-intercalated cells to α-intercalated and principal cells in culture. *Proc Natl Acad Sci USA* 89:5487-5491, 1992.

Fredin BL, Seiffert SC, Gelehrter TD: Dexamethasone-induced adhesion in hepatoma cells: The role of plasminogen activator. *Nature* 277:312-313, 1979.

Freshney RI: *Culture of Animal Cells, a manual of basic technique*. Third edition, John Wiley & Sons Inc., Toronto, p 200, 1994.

Fushimi K, Uchida S, Hara Y, Hirata y, Marumo F, Sasaki S: Cloning and expression of apical membrane water channel of rat kidney collecting tubule. *Nature Lond* 361:549-552, 1993.

Garcia I, Sordat B, Raucio-Farinon E, Dunand M, Kraehenbuhl JP, Diggelmann H: Establishment of two rabbit mammary epithelial cell lines with distinct oncogenic potential and differentiated phenotype after microinjection of transforming genes. *Mol Cell Biol* 6:1974-1982, 1986.

Geibel J, Giebisch G, Boron WF: Angiotensin II stimulates both Na^+-H^+ exchange and Na^+-HCO_3^- cotransport in the rabbit proximal tubule. *Proc Natl Acad Sci USA* 87:7917-7920, 1990.

Goldblatt H: The renal origin of hypertension. *Physiol Rev* 27:120-165, 1947.

Goldblatt H, Lynch J, Hanzal RF, Summerville WW: Studies on experimental hypertension. I. The production of persistent elevation of systolic blood pressure by means of renal ischemia. *J Exp Med* 59:347-379, 1934.

Gordon JA: Denaturation of Globular Proteins: Interaction of Guanidinium salts with three proteins. *Biochemistry* 11:1862-1870, 1972.

Goulian M: Initiation of the replication of single-stranded DNA by Escherichia coli DNA polymerase. *Cold Spring Harbor Symp Quant Biol* 33:11-20, 1969.

Graham Fl, Van der Eb AJ: A new technique for the assay of infectivity of human adenovirus 5 DNA. *Virology* 52:456-461, 1973.

Grantham JJ, Orloff J: Effect of prostaglandin E_1 on the permeability response of the isolated collecting tubule to vasopressin, adenosine 3', 5'-monophosphate, and Theophylline. *J Clin Invest* 47:1154-1161, 1968.

Griendling KK, Alexander RW: The Angiotensin (AT1) receptor. *Sem Nephrol* 13:558-566, 1993.

Grone HJ, Simon M, Fuchs E: Autoradiographic characterization of angiotensin receptor subtypes in fetal and adult human kidney. *Am J Physiol* 262:F326-F331, 1992.

Hagège J, Gabe M, Richet G: Scanning of the apical pole of distal tubular cells under differing acid-base conditions. *Kidney Int* 5:137-146, 1974.

Hamilton WG, Ham RG: Clonal growth of chinese hamster cell lines in protein-free media. *In Vitro* 13:537-547, 1977.

Harris, RC: Regulation of S6 kinase activity in renal proximal tubule. *Am J Physiol* 263:F127-F134, 1992.

Harris PJ: Regulation of proximal tubule function by angiotensin. *Clin Exp Pharm Phys* 19:213-222, 1992.

Hays RM, Ding G, Franki N: Morphological aspects of the action of ADH. *Kidney Int* 32:S51-S55, 1987.

Hébert RL, Jacobson HR, Breyer MD: PGE_2 inhibits AVP-induced water flow in cortical collecting ducts by protein kinase C activation. *Am J Physiol* 259:F318-F325, 1990.

Hébert RL, Jacobson HR, Breyer MD: Prostaglandin E_2 inhibits sodium transport in rabbit cortical collecting duct by increasing intracellular calcium. *J Clin Invest* 87:1992-1998, 1991.

Herter P, Laube G, Gronczewski J, Minuth WW: Silver-enhanced colloidal-gold labelling of rabbit kidney collecting-duct cell surfaces imaged by scanning electron microscopy. *J Microscopy* 171:107-115, 1993.

Holthöfer H: Cell type-specific glycoconjugates of collecting duct cells during maturation of the rat kidney. *Cell Tissue Res* 253:305-309, 1988.

Holthöfer H, Schulte BA, Pasternack G, Siegel EJ, Spice SS: Three distinct cell populations in rat kidney collecting duct. *Am J Physiol* 253:C323-C328, 1987.

Ichikawa I, Harris RC: Angiotensin actions in the kidney: Renewed insight into the old hormone. *Kidney Int* 40:583-596, 1991.

Imbert M, Chabardès D, Montegut M, Clique A, Morel F: Vasopressin dependent adenylate cyclase in single segments of rabbit kidney tubule. *Pfluger Arch* 357:173-186, 1975.

Imbert-Teboul M, Doucet A, Marsy S, Siaume-Perez S: Alterations in enzymatic activities along the rat collecting tubule in potassium depletion. *Am J Physiol* 253:F408-F417, 1987.

Jamous M, Koechlin N, Tauc M, Poujeol P, Rambourg A: Evolution of a cortical collecting tubule primary culture. *European J Cell Biol* 61:392-399, 1993.

Kaissling B, Kriz W: Structural analysis of the rabbit kidney, in *Advances in Anatomy Embryology and Cell Biology*, Springer Verlag, New York, Vol 56, p 89-100, 1979.

Karnovsky MJ: A formaldehyde-gluteraldehyde fixative of high osmolality for use in electron microscopy. *J Cell Biol* 27:137A, 1965.

Katzung BG: *Basic and Clinical Pharmacology*, fifth edition, Appleton and Lange, Norwalk, Connecticut, p 250, 1992.

Khandjian EW: Optimized hybridization of DNA blotted and fixed to nitrocellulose and nylon membranes. *Bio Tech* 5:165-169, 1987.

Kirk K: Binding and internalization of a fluorescent vasopressin analogue by collecting duct cells. *Am J Physiol* 255:C622-C632, 1988.

Kishore BK, Knepper MA: Vasopressin increases water permeability of kidney collecting duct by inducing translocation of aquaporin-CD water channels to plasma membrane. *Proc Natl Acad Sci USA*: 92:1013-1017, 1995.

Labarca C, Paigen K: A simple, rapid, and sensitive DNA assay procedure. *Anal Biochem* 102:344-342, 1980.

Lajeunesse D, Regnier L, Thales S, Hebert RL: Simultaneous isolation and biochemical characterization of connecting and collecting tubules by ficoll gradient. *Kidney Int* 47:306-311, 1995.

Lefurgey A, Tisher CC: Morphology of rabbit collecting duct. *Am J Anat* 155:111-124, 1979.

LeHir M, Kaissling B, Koeppen BM, Wade JB: Binding of peanut lectin to specific epithelial cell types in the kidney. *Am J Physiol* 242:C117-C120, 1982.

Lehrach H, Diamond D, Wozney JM, Boedtker H: RNA molecular weight determinations by gel electrophoresis under denaturing conditions, a critical reexamination. *Biochemistry* 16:4743-4751, 1977.

Levine DZ, Iacovitti M, Buckman S, Harrison V: In vivo modulation of rat distal tubule net HCO_3 flux by VIP, isoproterenol, angiotensin II, and ADH. *Am J Physiol* 266: F878-883, 1994.

Li L, Wang LP, Capparelli AW, Jo OD, Yanagawa N: Effect of luminal angiotensin II on proximal tubule fluid transport: role of apical phospholipase A_2. *Am J Physiol* 266:F202-F209, 1994.

Lotan R, Skutelsky E, Danon D, Sharon N: The purification, composition, and specificity of the anti-T lectin from peanut (*arachis hypogaea*). *J Biol Chem* 250:8518-8523, 1975.

Lui FY, Cogan MG: Angiotensin II stimulates early proximal bicarbonate reabsorption in the rat by decreasing cyclic adenosine monophosphate. *J Clin Invest* 84:83-91, 1989.

Ma T, Hasegawa H, Skach WR, Frigeri A, Verkman AS: Expression, functional analysis, and in situ hybridization of a cloned rat kidney collecting duct water channel. *Am J Physiol* 266:C189-C197, 1994.

Markwell MAK, Haas SM, Bieber LL, Tolbert NE: A modification of the Lowry procedure to simplify protein determination in membrane and lipoprotein samples. *Anal Biochem* 87:206-210, 1978.

McGadey J: A tetrazolium method for non-specific alkaline phosphatase. *Histochim* 23:180-184, 1970.

McLean JS, Frame MC, Freshney RI, Vaughan PFT, Mackie AE: Phenotypic modification of human glioma and non-small cell lung carcinoma by glucocorticoids and other agents. *Anticancer Res* 6:1101-1106, 1986.

McKinney TD, Burg MB: Bicarbonate transport by rabbit cortical collecting tubules. Effect of acid and alkali loads in vivo on transport in vitro. *J Clin Invest* 60:766-768, 1977.

Miller K: Gel electrophoresis of RNA. *Bethesda Res Lab Focus* 9:14-17, 1987.

Minuth WW, Gross P, Gilbert P, Kashgarian M: Expression of the α-subunit of Na/K-ATPase in renal collecting duct epithelium during development. *Kidney Int* 31:1104-1112, 1987.

Minuth WW, Fietzek W, Kloth S, Aigner J, Herter P, Röckl W, Kubitza M, Stökl G, Dermietzel R: Aldosterone modulates PNA binding cell isoforms within renal collecting duct epithelium. *Kidney Int* 44:537-544, 1993.

Morel F, Charbadès D, Imbert M, Montegut M, Clique A: Functional segmentation of the rabbit distal tubule by microdetermination of hormone-dependent adenylate cyclase activity. *Kidney Int* 9:264-277, 1976.

Mortell KH, Marmorstein AD, Cramer EB: Fetal bovine serum and other sera used in tissue culture increase epithelial permeability. *In Vitro C Dev Biol* 29A:235-238, 1993.

Mujais SK: Collecting duct changes in potassium depletion: effects of ACE inhibition. *Am J Physiol* 266:F419-F424, 1994.

Mujais SK, Chen Y, Nora NA: Discordant aspects of aldosterone resistance in D depletion. *Am J Physiol* 262:F972-F979, 1992.

Mujais SK, Kauffman S, Katz AI: Angiotensin II Binding Sites in Individual Segments of the Rat Nephron. *J Clin Invest* 77:315-318, 1986.

Nelson RD, Guo XL, Masood K, Brown D, Kalkbrenner M, Gluck S: Selectively amplified expression of an isoform of the vacuolar H^+-ATPase 56-kilodalton subunit in renal intercalated cells. *Proc Natl Acad Sci USA* 89:3541-3545, 1992.

Nuyts GD, Verpooten GF, DeBroe ME: Intestinal alkaline phosphatase as an indicator of effects on the S3-segment of the human proximal tubule. *Eur J Clin Chem Clin Biochem* 30:713-715, 1992.

O'Neil RG, Hayhurst RA: Functional differentiation of cell types of cortical collecting duct. *Am J Physiol* 248:F449-F453, 1985.

Page IH, Helmer OM: A crystalline pressor substance (angiotonin) resulting from the reaction between renin and renin activator. *J Exp Med* 71:29-42, 1940.

Prié D, Dussaule JC, Lelongt B, Geniteau-Legendre M, Chatelet F, Cassingena R, Vandewalle A, Ronco PM: Principal cell-specific antigen and hormonal regulatory network in RC.SVtsA58 cell line. *Am J Physiol* 266:C1628-C1638, 1994.

Rabito CA, Tchao R, Valentich J, Leighton J: Effect of cell substratum interaction of hemicyst formation by MDCK cells. *In Vitro* 16:461-468, 1980.

Raymond KK, Davidson K, McKinney T: In vivo and in vitro studies of urinary concentrating ability in potassium depleted rabbits. *J Clin Invest* 76:561-566, 1985.

Reed KC, Mann DA: Rapid transfer of DNA from agarose gels to nylon membranes. *Nucleic Acids Res* 13:7207-7210, 1985.

Ridderstrale Y, Kashgarian M, Koeppen B, Glebish G, Stetson D, Ardito T, Stanton B: Morphological heterogeneity of the rabbit collecting duct. *Kidney Int* 34:655-670, 1988.

Satlin LM, Schwartz GJ: Cellular remodeling of HCO_3^--secreting cells in rabbit renal collecting duct in response to and acidic environment. *J Cell Biol* 109:1279-1288, 1989.

Schafer JA, Troutman SL, Schlatter E: Vasopressin and mineralocorticoid increase apical membrane driving force for K^+ secretion in rat CCD. *Am J Physiol* 258:F199-F210, 1990.

Schuster VL, Bonsib SM, Jennings ML: Two types of collecting duct mitochondria-rich (intercalated) cells: Lectin and band 3 cytochemistry. *Am J Physiol* 251:C347-C355, 1986.

Schuster VL: Bicarbonate reabsorption and secretion by the cortical and outer medullary collecting tubule. *Semin Nephrol* 10:139-147, 1990.

Schuster VL: Colocalization of H^+-ATPase and band 3 anion exchanger in rabbit collecting duct intercalated cells. *Am J Physiol* 260:F506-F517, 1991.

Shuster VL: Function and regulation of collecting duct intercalated cells. *Annu Rev Physiol* 55:267-88, 1993.

Schwartz GJ, Barasch J, Al-Awquati Q: Plasticity of functional epithelial polarity. *Nature Lond* 318:368-371, 1985.

Seed B: Attachment of nucleic acids to nitrocellulose and iasonim-substituted supports. *In Genetic engineering: Principles and methods,* Plenum Publishing, New York, vol 4, p 91, 1973.

Skeggs LT, Marsh WH, Kahn JR, Shumway NP: The purification of hypertensin I. *J Exp Med* 100:363-370, 1954.

Silver RB, Frindt G: Functional identification of H^+-K^+-ATPase in intercalated cell of cortical collecting tubule. *Am J Physiol* 264:F259-F266, 1993.

Smith JB, Smith L, Brown ER, Barnes D, Sabir MA, Davis JS, Farese RV: Angiotensin II rapidly increases phosphatidate-phosphoinositide synthesis, phosphoinositide hydrolysis and calcium mobilization in cultured arterial muscle cells. *Proc Natl Acad Sci USA* 81;7812-7816, 1984.

Snyder HM, Noland TD, Breyer MD: cAMP-dependent kinase mediates hydroosmotic effect of vasopressin in collecting duct. *Am J Physiol* 263:C147-C153, 1992.

Sonnenburg WK, Smith WL: Regulation of cyclic AMP metabolism in rabbit cortical collecting tubule cells by prostaglandins. *J Biol Chem* 263:6155-6160, 1988.

Southern EM: Detection of specific sequences among DNA fragments separated by gel electrophoresis. *J Mol Biol* 98:503-517, 1975.

Speirs V, Ray KP, Freshney RI: Paracrine control of differentiation in the alveolar carcinoma, A549, by human foetal lung fibroblasts. *Br J Cancer* 64:693-699, 1991.

Stetson DL, Wade JB, Giebisch G: Morphologic alterations in the rat medullary collecting duct following potassium depletion. *Kidney Int* 17:45-56, 1980.

Stokes JB: Ion transport by the collecting duct. *Sem Nephrol* 13:202-212, 1993.

Stone DK, Seldin DW, Kokko JP, Jacobson HR: Mineralocorticoid modulation of rabbit medullary collecting duct acidification. A sodium-independent effect. *J Clin Invest* 72:77-83, 1983.

Stoos BA, Náray-Fejes-Tóth A, Carretero OA, Ito S, Fejes-Tóth G: Characterization of a mouse cortical collecting duct cell line. *Kidney Int* 39:1168-1175, 1991.

Sumners C, Tang W, Zelezna B, Raizada MK: Angiotensin II receptor subtypes are coupled with distinct signal-transduction mechanisms in neuron and astrocytes from rat brain. *Proc Natl Acad Sci USA* 88:7567-7571, 1991.

Tanner C, Frambach DA, Misfeldt DS: Biophysics of domes formed by the renal cell line Madin-Darby canine kidney. *Federation Proc* 43:2217-2220, 1984.

Tauc M, Koechlin N, Jamous M, Ouaghi EM, Gastineau M, Le Moal C, Poujeol P: Principal and intercalated cells in primary cultures of rabbit renal collecting tubules revealed by monoclonal antibodies. *Biol Cell* 76:555-565, 1992.

Tigerstedt R, Bergman PG: Niere und Kreislauf. *Scand Arch Physiol* 8:223-271, 1898.

Timmermans PBMWM, Wong PC, Chiu AT, Herblin WF: Nonpeptide angiotensin II receptor antogonists. *TIPS* 12:55-62, 1991.

Timmermans PBMWM, Wong PC, Chiu AT, Herblin WF, Benfield P, Carini DJ, Lee RJ, Wexler RR, Saye JOM, Smith RD: Angiotensin II receptors and angiotensin II receptor antagonists. *Pharm Rev* 45:205-251, 1993.

Tojo A, Tisher CC, Madsen KM: Angiotensin II regulates H^+-ATPase activity in the rat cortical collecting duct (CCD). *Am J Physiol* 267:F1045-F1051, 1994.

Torikai S, Kurokawa K: Effect of PGE_2 on vasopressin-dependent cell cAMP in isolated single nephron segments. *Am J Physiol* 245:F558-F566, 1983.

Valenti G, Verbavatz JM, Sabolic I, Ausiello DA, Verkman AS, Brown D: A CHIP28/MIP26-related protein (BLIP) in basolateral membranes of kidney collecting duct principal cells and gastric parietal cells. *Am J Physiol* 267:C812-C820, 1994.

Van Aldesberg, Edwards JC, Herzlinger D, Cannon C, Rater M, Al-Awqati Q: Isolation and culture of HCO_3^- secreting intercalated cells. *Am J Physiol* 256:C1004-C1011, 1989.

Van Aldesberg J, Edwards JC, Takito J, Kiss B, Al-Awqati Q: An induced extracellular matrix protein reverses the polarity of band 3 in intercalated epithelial cells. *Cell* 76:1053-1061, 1994.

Verlander JW, Madsen KM, and Tisher CC: Effect of acute respiratory acidosis on two populations of intercalated cells in rat cortical collecting duct. *Am J Physiol* 253:F1142-F1156, 1987.

a) **Verlander JW, Madsen KM, Stone DK, Tisher CC:** Ultrastructural localization of H^+ATPase in Rabbit Cortical Collecting Duct. *J Am Soc Nephrol* 4:1546-1557, 1994.

b) **Verlander JW, Madsen KM, Cannon JK, Tisher CC:** Activation of acid-secreting intercalated cells in rabbit collecting duct with ammonium chloride loading. *Am J Physiol* 266:F633-F645, 1994.

Wade JB, O'Neil RG, Pryor J, Boulpaep EL: Modulation of cell membrane area in renal collecting tubules by corticosteroid hormones. *J Cell Biol* 81:439-445, 1979.

Wang W, Sackin H, Giebisch G: Renal potassium channels and their regulation. *Annu Rev Physiol* 54:81-96, 1992.

Wang T, Chan YL: The role of phosphoinositide turnover in mediating the biphasic effect of angiotensin II on renal tubular transport. *J Pharmacology Therapeutics* 256:309-317, 1991.

Welling LW, Evan AP, Welling DJ: Shape of cells and extracellular channels in rabbit cortical collecting ducts. *Kidney Int* 20:211-222, 1981.

Wolf G, Zahner G, Mondorf U, Schoeppe W, Stahl RA: Angiotensin II stimulates cellular hypertrophy of LLC-PK1 cells through the AT_1 receptor. *Nephrol Dialysis Transpl* 8:128-133, 1993.

Woodward DF, Protzman CE, Krauss AHP, Williams LS: Identification of 19 (R)-OH Prostaglandin E_2 as a selective prostanoid EP_2 receptor agonist. *Prostaglandins* 46:371-383, 1993.